

Robust identification and fault diagnosis based on uncertain multiple input–multiple output linear parameter varying parity equations and zonotopes

Joaquim Blesa^a, Vicenç Puig^{a,b} and Jordi Saludes^a

^aAdvanced Control Systems Group, Universitat Politècnica de Catalunya,

Pau Gargallo, 5, 08028 Barcelona, Spain. (e-mail: joaquim.blesa@upc.edu)

^bIRI Institut de Robòtica i Informàtica Industrial (CSIC-UPC), Carrer Llorens Artigas, 4-6, 08028 Barcelona, Spain

Abstract: We present a robust fault diagnosis method for uncertain multiple input–multiple output (MIMO) linear parameter varying (LPV) parity equations. The fault detection methodology is based on checking whether measurements are inside the prediction bounds provided by the uncertain MIMO LPV parity equations. The proposed approach takes into account existing couplings between the different measured outputs. Modelling and prediction uncertainty bounds are computed using zonotopes. Also proposed is an identification algorithm that estimates model parameters and their uncertainty such that all measured data free of faults will be inside the predicted bounds. The fault isolation and estimation algorithm is based on the use of residual fault sensitivity. Finally, two case studies (one based on a water distribution network and the other on a four-tank system) illustrate the effectiveness of the proposed approach.

Keywords: Fault Detection, Isolation and Estimation. Linear Parameter Varying Model, Sensitivity Matrix.

1. INTRODUCTION

Model-based fault diagnosis is based on the use of mathematical models of the monitored system. Currently, most of the existing approaches that have been investigated and developed over the last few years are based on linear models (Gertler, 1998)(Chen and Patton, 1998)(Isermann, 2006)(Blanke *et al.*, 2006)(Ding, 2008). However, physical systems are inherently non-linear. This has motivated the interest of researchers in the development and application of non-linear FDI methodologies (Bokor *et al.*, 2002). LPV models can be used to efficiently represent some nonlinear systems (Shamma and Cloutier, 1993). This is the reason why *Fault Detection and Isolation* (FDI) research community has recently addressed the development of

model-based methods using the LPV approach (see Bokor, 2009 for a recent survey). But, even with the use of LPV models, modelling errors are present. Reliability and performance of fault diagnosis algorithms depend on the quality of the model used. Thus, since modelling errors introduce uncertainty in the model, they interfere with the fault detection. A fault detection algorithm able to handle uncertainty is called *robust* and its *robustness* is the degree of sensitivity to faults compared to the degree of sensitivity to uncertainty. The effect of noise on the model-based fault detection is well understood using statistical approaches (Basseville and Nikiforov, 1993). However, in many situations, the random nature of noise is unknown what makes difficult the use of statistical methods and has led to an alternative description of the noise based on what is known as “*unknown but bounded noise*” description (Milanese *et al.*, 1996). Moreover, not only noise but also modelling errors should be taken into account. Modelling errors inclusion in the statistical methods is far from being trivial. For all these reasons, the research on robust fault detection methods that requires only knowledge about bounds in noise and parameters (modelling errors) has been very active in the FDI community (Fagarasan *et al.*, 2004; Puig *et al.*, 2008; Sainz *et al.*, 2002; Ploix and Adrot, 2006; Reppa and Tzes 2009; Combastel and Raka 2009; Combastel *et al.*, 2008; Raissi *et al.*, 2010). These methods, known as *set-membership*, follow the *passive robust approach* (Chen and Patton, 1999) by enhancing the fault detection robustness at the decision-making stage using an adaptive threshold. This adaptive threshold is generated by considering the set of model trajectories that can be obtained by varying the uncertain parameters within their intervals.

The contribution of this paper is to present a fault diagnosis method for systems that can be described by MIMO LPV models with a set-membership description of the noise and parametric uncertainty. The proposed approach covers fault detection, isolation and estimation stages. The fault detection methodology uses the *parity equation formulation* (see Gertler (1998)) expressing the model in regressor (ARX) form. Fault detection relies on comparing on-line the real system behaviour of the monitored system obtained by means of sensors with the estimated behaviour using the MIMO LPV model including the effects of noise and parametric uncertainty. In particular, the parametric uncertainty bounded by a zonotope is propagated to the residuals determining their alarm limits bounded by a zonotope as well. When the residuals are outside of the zonotope that defines the alarm limits, it is argued that model uncertainty alone can not explain the residual and it is assumed that a fault could have occurred. In this way, the robustness of the fault detection approach is achieved in a passive way contrarily to the active approaches that try to decouple the effect of the uncertainty on the residual (Chen and Patton, 1999). The passive approach has the drawback that faults that produce a residual deviation smaller than the residual uncertainty due to parameter uncertainty will not be detected (missed alarms). But on the other hand, if noise and parametric uncertainty bounds are correctly tuned, using for example the model identification algorithm proposed in this paper, false alarms are avoided.

Regarding fault detection, the proposed approach extends the results of Adrot *et al.* (2002) that uses parallelotopes to represent parametric uncertainty and considers static LTI systems.

This paper also deals with the uncertain MIMO LPV model calibration that allows to find the uncertain parameter set considering that can be bounded by a zonotope extending the ideas proposed by Ploix *et al.* (1999) for static LTI systems and intervals for modelling parametric uncertainty. Finally, a fault isolation approach, alternative to the classic one based on binary fault signatures, is proposed. The proposed method uses the residual fault sensitivity to improve the isolation results as seminally suggested in Meseguer *et al.*, (2010) but formulating instead the fault isolation and estimation as an optimization problem. The residual fault sensitivity concept has been introduced by Gertler (1998) and Isermann (2006) to characterize the performance of the fault detection but they have not used it for fault isolation. In Blanke *et al.* (2006), the idea of using the transfer function that relates residual and faults (what is called residual fault sensitivity in this paper) is suggested to estimate the fault size by means of the pseudoinverse in case of LTI systems. Here, the proposed fault estimation approach based on optimization allows to estimate the fault without using the pseudoinverse and it can be applied to LPV systems.

The structure of this paper is the following: *Section 2* introduces LPV parity equations with uncertainty, the consistency test used for fault detection as well as provides an overview of the proposed fault diagnosis approach. In *Section 3*, a parameter estimation procedure is described that allows bounding the parametric uncertainty using zonotopes and data from fault-free scenarios. *Section 4* presents a fault detection methodology that relies on the use of the uncertain LPV parity equations and zonotopes. *Section 5* presents the fault isolation and estimation methodology that makes use of residual fault sensitivity analysis. Finally, in *Sections 6 and 7*, a piece of water distribution network and a four tank system (a well known control benchmark) are used to assess the validity of the proposed approach.

2. OVERVIEW OF THE PROPOSED FAULT DIAGNOSIS APPROACH

2.1 LPV parity equations with uncertainty

In this paper, the system to be monitored is assumed that can be described by a MIMO LPV model*

$$\mathbf{y}(k) = \mathbf{\Phi}(k)\boldsymbol{\theta}(\mathbf{p}_k) + \mathbf{e}(k) = \hat{\mathbf{y}}(k) + \mathbf{e}(k) \quad (1)$$

where

- $\mathbf{y}(k)$ is the output vector of dimension $n_y \times 1$.

- $\Phi(k)$ is the regressor matrix of dimension $n_y \times n_\theta$ which can contain any function of inputs $\mathbf{u}(k)$ and outputs $\mathbf{y}(k)$.
- $\mathbf{p}_k \triangleq \mathbf{p}(k)$ is a vector of measurable process variables of dimension $n_p \times 1$ that defines the system operating point.
- $\boldsymbol{\theta}(\mathbf{p}_k) \in \Theta_k$ is the LPV parameter vector of dimension $n_\theta \times 1$ whose values can vary according to the system operating point following some known function $g(\mathbf{p}_k)$, usually named as *scheduling function*.
- $\mathbf{e}(k)$ is a vector of dimension $n_y \times 1$ that contains the sensor additive noises whose components are bounded by constant bounds: $|e_i(k)| \leq \sigma_i, i = 1, \dots, n_y$.

There are several ways to obtain an LPV model either from the system non-linear equations, as e.g., using a state transformation (Shamma and Cloutier, 1993) or embedding non-linearities inside the LPV parameters (Kwiatkowski *et al.*, 2006), or through LPV identification methods (Bamieh and Giarré, 2002).

In this paper, the uncertain parameter set Θ_k is described by a zonotope centered in the nominal LPV model:

$$\Theta_k = \boldsymbol{\theta}^0(\mathbf{p}_k) \oplus \mathbf{H} \mathbb{B}^n = \{ \boldsymbol{\theta}^0(\mathbf{p}_k) + \mathbf{H}\mathbf{z} : \mathbf{z} \in \mathbb{B}^n \} \quad (2)$$

where

- $\boldsymbol{\theta}^0(\mathbf{p}_k) \in \mathbb{R}^{n_\theta}$ is the centre of the zonotope and corresponds to the nominal LPV model.
- $\mathbf{H} \in \mathbb{R}^{n_\theta \times n}$ is the shape of the zonotope (usually $n \geq n_\theta$ and as the bigger n is the more complicated relations between uncertain parameters can be taken into account).
- $\mathbb{B}^n \in \mathbb{R}^{n \times 1}$ is a unitary box composed by n unitary interval vectors, i.e. $\mathbb{B} = [-1, 1]$.
- \oplus denotes the Minkowski sum.

2.2 Consistency test

Given the MIMO LPV model (1), the output measurement vector $\mathbf{y}(k)$ will be consistent with the output predicted by the model if

$$\mathbf{y}(k) \in \Upsilon(k) \quad (3)$$

where

$$\Upsilon(k) = \hat{\mathbf{Y}}(k) \oplus \mathbf{E} \mathbb{B}^{n_y} \quad (4)$$

with

* An LPV model has linear structure with parameters that are not constant but vary with the system operating point. The variation of parameters with the operating point is described by some known function. The operating point can be characterized through some measured variable: external or internal to the system. In case that an internal variable of the model is used the model is named as *quasi-LPV* (Shamma and Cloutier, 1993).

$$\hat{\mathbf{Y}}(k) = \{ \hat{\mathbf{y}}(k) = \mathbf{\Phi}(k)\boldsymbol{\theta}(\mathbf{p}_k), \boldsymbol{\theta}(\mathbf{p}_k) \in \Theta_k \} \quad (5)$$

and $\mathbf{E} = \text{diag}(\sigma_1, \dots, \sigma_{n_y})$. This means that output measurement vector $\mathbf{y}(k)$ is inside the set of possible outputs that can be obtained using model (1), parameter uncertainty (2) and noise bounds.

This approach was first suggested by Ploix *et al.* (1999) in the context of fault detection for SISO LTI systems, and later developed by Calafiore *et al.* (2002) and Campi *et al.* (2009). Adrot *et al.* (2002) extended this approach to MIMO LTI systems. In the following, this approach is extended to MIMO LPV systems with uncertain parameters bounded by zonotopes.

When the uncertain parameter set Θ_k is described by means of a zonotope, as in (2), (5) can be rewritten as follows

$$\hat{\mathbf{Y}}(k) = \mathbf{\Phi}(k)\boldsymbol{\theta}^0(\mathbf{p}_k) \oplus \mathbf{\Phi}(k)\mathbf{H}\mathbb{B}^n \quad (6)$$

Consequently, $\mathbf{Y}(k)$ leads to

$$\mathbf{Y}(k) = \hat{\mathbf{y}}^0(k) \oplus \hat{\mathbf{\Gamma}}(k) \quad (7)$$

where

$$\hat{\mathbf{y}}^0(k) = \mathbf{\Phi}(k)\boldsymbol{\theta}^0(\mathbf{p}_k) \quad (8)$$

and

$$\hat{\mathbf{\Gamma}}(k) = (\mathbf{\Phi}(k)\mathbf{H} \quad \mathbf{E}) \mathbb{B}^{n+n_y} \quad (9)$$

Notice that $\mathbf{Y}(k)$ is a zonotope centred in the nominal output estimation $\hat{\mathbf{y}}^0(k)$ and with a shape defined by $\hat{\mathbf{\Gamma}}(k)$. Thus, condition (3) can be rewritten as

$$\mathbf{y}(k) - \hat{\mathbf{y}}^0(k) \in \hat{\mathbf{\Gamma}}(k) \quad (10)$$

2.3 Overview of the proposed fault diagnosis approach

Using the LPV uncertain parity equations introduced in *Section 2.1*, as well as the consistency test presented in *Section 2.2*, a set of algorithms that allow fault detection (*Section 4*), isolation and estimation (*Section 5*) will be presented in this paper. Fig. 1 presents how the different algorithms interact. The measured system output is compared with the nominal predicted output using the LPV nominal model (1) by generating a residual. This residual is evaluated using the consistency test presented in previous section that considers the parametric uncertainty and additive noise bounds. If an inconsistency is detected a fault is indicated. Then, the fault isolation and estimation block is activated and the most probable fault and its magnitude are determined. An algorithm to estimate the LPV parameter and their uncertainty of parity equations (1) are also proposed (*Section 3*) that also relies on the consistency test presented in *Section 2.2*.

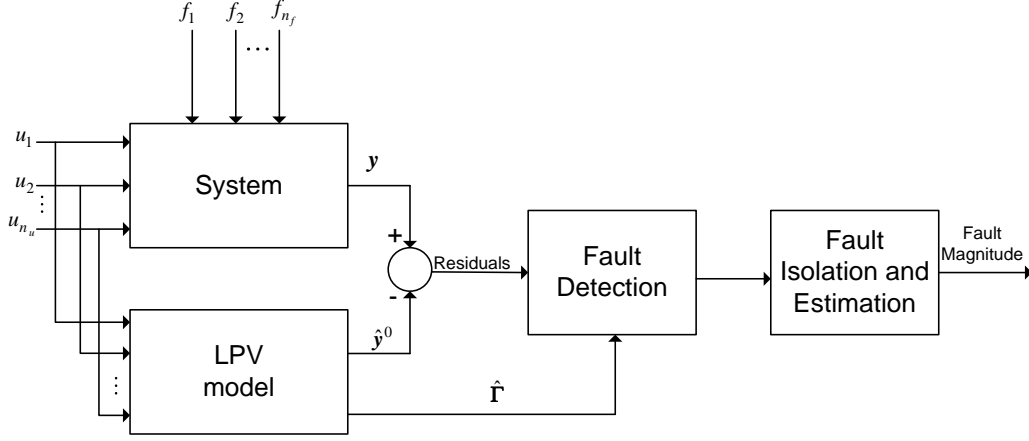


Figure 1: Scheme of fault detection, isolation and estimation procedure

3. UNCERTAIN PARAMETER ESTIMATION

In practice, nominal LPV parameters $\theta^0(\mathbf{p}_k)$ could be obtained using LPV identification algorithms as the ones proposed by (Bamieh and Giarré, 2002) and real data or by the physical knowledge of the system. However, as a result of this process, some modelling uncertainty (2) in the LPV parameters appears. Thus, additionally to estimate the nominal LPV parameters $\theta^0(\mathbf{p}_k)$, the uncertainty in the parameters should be estimated. This is especially important when the model should be used in robust fault diagnosis.

Let us consider that a sequence of M regressor matrix values $\Phi(k)$ and output measurements $\mathbf{y}(k)$ in a fault free scenario is available, the model of the system to be monitored can be parameterized as in (1) and the parameter set Θ_k can be described as a zonotope (2). The aim is to estimate parameter uncertainty set Θ_k defined by the matrix \mathbf{H} in such a way that all measured data in a fault free scenario satisfy condition (10). This condition can be applied to every component through the following n_y equations

$$\begin{aligned} y_1(k) - \hat{y}_1^0(k) &= \boldsymbol{\varphi}_1(k) \mathbf{H} \mathbf{z}(k) + e_1(k) \\ &\vdots \\ y_{n_y}(k) - \hat{y}_{n_y}^0(k) &= \boldsymbol{\varphi}_{n_y}(k) \mathbf{H} \mathbf{z}(k) + e_{n_y}(k) \end{aligned} \quad (11)$$

with $\boldsymbol{\varphi}_i(k) \in \mathbb{R}^{1 \times n_\theta}$ $i = 1, \dots, n_y$ and $\Phi(k) = \begin{pmatrix} \boldsymbol{\varphi}_1(k) \\ \vdots \\ \boldsymbol{\varphi}_{n_y}(k) \end{pmatrix}$ and $\mathbf{z}(k) \in \mathbb{B}^n$, $(e_1, \dots, e_{n_y})^t \in \mathbf{E} \mathbb{B}^{n_y}$

the discarding procedure boils down to remove the N data that provides a value of λ exceptionally large, and repeating the identification with the remaining $M - N$ data.

4. FAULT DETECTION METHODOLOGY

4.1 Fault Detection Procedure

The fault detection methodology is based on the residual evaluation obtained from the difference between measurements and LPV model prediction using (1)

$$\mathbf{r}(k) = \mathbf{y}(k) - \hat{\mathbf{y}}(k) - \mathbf{e}(k) = \mathbf{y}(k) - \Phi(k)\boldsymbol{\theta}(\mathbf{p}_k) - \mathbf{e}(k) \quad (13)$$

that corresponds to a *MA parity equation* (Gertler, 1998). Ideally, when modelling errors and noise are neglected, residual (13) should be zero in a fault-free scenario and different from zero, otherwise. However, because of modelling errors and noise, residual can be different from zero in a non faulty scenario. In order to take into account uncertainty in parameters and additive noise, the effects of these uncertainties will be propagated to the residual defining the region of admissible residuals. A fault will be detected when zero does not belong to this set. Then, the consistency test (10) is equivalent to check the following fault detection test

$$\mathbf{0} \in \Gamma(k) \quad (14)$$

where

$$\Gamma(k) = \left\{ \begin{array}{l} \mathbf{r}(k) = \mathbf{y}(k) - \Phi(k)\boldsymbol{\theta}(\mathbf{p}_k) - \mathbf{e}(k), \\ \boldsymbol{\theta}(\mathbf{p}_k) \in \Theta_k, \mathbf{e}(k) \in \mathbb{E}\mathbb{B}^{n_y} \end{array} \right\}$$

and $\mathbf{0}$ is a vector ($n_y \times 1$) of zeros $\mathbf{0} = (0 \cdots 0)^t$.

Taking into account (1) and (2), $\Gamma(k)$ can be parameterized as a zonotope

$$\Gamma(k) = (\mathbf{y}(k) - \hat{\mathbf{y}}^0(k)) \oplus \hat{\Gamma}(k) \quad (15)$$

where $\hat{\mathbf{y}}^0(k)$ and $\hat{\Gamma}(k)$ are defined as in (8) and (9). Then, test (14) is equivalent to test (6) and involves checking if the point $\mathbf{0}$ belongs to the zonotope $\Gamma(k)$. The fault detection test (14), considering matrix \mathbf{H} known (calibrated as it was proposed in Section 3), can be implemented by determining if the constraint satisfaction problem, named as *Problem 2*, is feasible.

Problem 2: “Fault Detection Test”

$$\begin{aligned}
 & y_1(k) - \hat{y}_1^0(k) - \boldsymbol{\varphi}_1(k) \mathbf{H} \mathbf{z}(k) - e_1(k) = 0 \\
 & \quad \vdots \\
 & y_{n_y}(k) - \hat{y}_{n_y}^0(k) - \boldsymbol{\varphi}_{n_y}(k) \mathbf{H} \mathbf{z}(k) - e_{n_y}(k) = 0 \\
 & \mathbf{z}(k) \in \mathbb{B}^n \quad \text{and} \quad (e_1, \dots, e_{n_y})^t \in \mathbf{E} \mathbb{B}^{n_y}
 \end{aligned}$$

Remark 3. For every instant k , the feasibility of *Problem 2* can be efficiently verified solving a linear programming problem without objective function.

Remark 4. The identification algorithm, described in *Section 3*, should deliver a model and an uncertainty parameter set that should include any healthy behaviour of the system. This only could be achieved if a large and rich enough (from the identifiability point of view) data set is used. In this case, the probability of false alarm applying fault detection test defined in *Problem 2* should be zero as already discussed in the introduction. However, according to (Campi *et al.*, 2009), when using a finite number of M data, the inclusion of all healthy behaviours can only be guaranteed with some confidence degree opening the possibility to have some false alarm. The probability of false alarm would even be increased if data, classified as possible outliers (see *Remark 2*), are discarded in identification process following the procedure described in (Campi *et al.*, 2009). Using the results presented in this reference, the probability of false alarm could even be quantified. However, in this work, this is considered as possible further research.

4.2 Fault Sensitivity

In fault detection, two kinds of faults are typically considered: additive faults (affecting input/output sensors and actuators) and multiplicative faults (in parameters) (Gertler, 1998). Including both types of faults in the system (1), residuals (13) can be approximated, neglecting the terms in the Taylor series corresponding to the second and higher order derivatives with respect to the fault, as follows

$$r_i(k) = y_i(k) - \hat{y}_i(k) - e_i(k) \approx f_{y_i} - \mathbf{f}_y^t \left(\mathbf{F}_{y\boldsymbol{\varphi}_i} \boldsymbol{\theta}(\mathbf{p}_k) + \mathbf{F}_{y\boldsymbol{\varphi}_i'} \boldsymbol{\varphi}_i^t(k) \right) - \mathbf{f}_u^t \left(\mathbf{F}_{u\boldsymbol{\varphi}_i} \boldsymbol{\theta}(\mathbf{p}_k) + \mathbf{F}_{u\boldsymbol{\varphi}_i'} \boldsymbol{\varphi}_i^t(k) \right) + \boldsymbol{\varphi}_i(k) \mathbf{f}_{\boldsymbol{\theta}} \quad \forall i = 1, \dots, n_y \quad (16)$$

where

- \mathbf{f}_y (vector $n_y \times 1$) and \mathbf{f}_u (vector $n_u \times 1$) are output and input faults (additive faults)
- f_{y_i} is an additive fault in the i^{th} sensor output (the i^{th} component of the vector \mathbf{f}_y)
- $\mathbf{f}_{\boldsymbol{\theta}}$ (vector $n_{\boldsymbol{\theta}} \times 1$) are the parametric faults (multiplicative faults)

with

$$F_{y\varphi_i}(q^{-1}) = \begin{pmatrix} \frac{\partial \varphi_i}{\partial f_{y_1}} \\ \vdots \\ \frac{\partial \varphi_i}{\partial f_{y_{n_y}}} \end{pmatrix}, F_{u\varphi_i}(q^{-1}) = \begin{pmatrix} \frac{\partial \varphi_i}{\partial f_{u_1}} \\ \vdots \\ \frac{\partial \varphi_i}{\partial f_{u_{n_u}}} \end{pmatrix}$$

$$F_{y\theta'}(q^{-1}, \theta(\mathbf{p}_k), \mathbf{f}) = \begin{pmatrix} \frac{\partial \theta_1(\mathbf{p}_k)}{\partial f_{y_1}} & \dots & \frac{\partial \theta_{n_0}(\mathbf{p}_k)}{\partial f_{y_1}} \\ \vdots & \vdots & \vdots \\ \frac{\partial \theta_1(\mathbf{p}_k)}{\partial f_{y_{n_y}}} & \dots & \frac{\partial \theta_{n_0}(\mathbf{p}_k)}{\partial f_{y_{n_y}}} \end{pmatrix} \text{ and } F_{u\theta'}(q^{-1}, \theta(\mathbf{p}_k), \mathbf{f}) = \begin{pmatrix} \frac{\partial \theta_1(\mathbf{p}_k)}{\partial f_{u_1}} & \dots & \frac{\partial \theta_{n_0}(\mathbf{p}_k)}{\partial f_{u_1}} \\ \vdots & \vdots & \vdots \\ \frac{\partial \theta_1(\mathbf{p}_k)}{\partial f_{u_{n_u}}} & \dots & \frac{\partial \theta_{n_0}(\mathbf{p}_k)}{\partial f_{u_{n_u}}} \end{pmatrix}$$

Notice that $F_{y\varphi_i}$ and $F_{u\varphi_i}$ matrices, with dimensions $n_y \times n_0$ and $n_u \times n_0$ respectively, are functions of the shift operator q^{-1} whose coefficients are constants. $F_{y\theta'}$ and $F_{u\theta'}$ matrices, with dimensions $n_y \times n_0$ and $n_u \times n_0$ respectively, are functions of the shift operator q^{-1} as well.

Remark 5. Coefficients of matrices $F_{y\theta'}$ and $F_{u\theta'}$ may depend on faults \mathbf{f} because faults could affect the scheduling variables \mathbf{p}_k in LPV parameters $\theta(\mathbf{p}_k)$. In this way the effect of faults in the scheduling variables could be characterized.

Remark 6. In case of *Linear Time Invariant* (LTI) systems, residual expression (17) is exact, because the second and higher derivative terms are zero, and $F_{y\theta'} = F_{u\theta'} = \mathbf{0}$ (see Gertler, 1998).

Residuals (16) can be expressed in a compact form using the fault sensitivity transfer function matrix (Isermann, 2006), defined as

$$\mathbf{r}(k) \simeq \mathbf{S}(q^{-1}, \theta(\mathbf{p}_k), \mathbf{f}) \mathbf{f}(k) \quad (17)$$

where

- $\mathbf{f}(k)$ is the vector of possible faults of dimension $n_f \times 1$

- $\mathbf{S}(q^{-1}, \theta(\mathbf{p}_k), \mathbf{f})$ is the fault sensitivity matrix of dimension $n_y \times n_f$ that can be calculated as

$$\mathbf{S}(q^{-1}, \theta(\mathbf{p}_k), \mathbf{f}) = \frac{\partial \mathbf{r}}{\partial \mathbf{f}} = \begin{pmatrix} \frac{\partial \mathbf{r}}{\partial f_1} & \dots & \frac{\partial \mathbf{r}}{\partial f_{n_f}} \end{pmatrix} \quad (18)$$

considering additive and multiplicative faults as in (16) and introducing the vector of faults of dimension $1 \times n_f$ with

$$n_f = n_y + n_u + n_0$$

$$\mathbf{f}(k) = \left(f_{y_1}, \dots, f_{y_{n_y}}, f_{u_1}, \dots, f_{u_{n_u}}, f_{\theta_1}, \dots, f_{\theta_{n_\theta}} \right)^t$$

Then, residual sensitivities to faults can be computed as follows

$$\frac{\partial \mathbf{r}}{\partial f_1} = \frac{\partial \mathbf{r}}{\partial f_{y_1}} = \begin{pmatrix} 1 - \mathbf{F}_{y_1 \phi_1} \boldsymbol{\theta} - \mathbf{F}_{y_1 \theta^t} \phi_1 \\ -\mathbf{F}_{y_1 \phi_2} \boldsymbol{\theta} - \mathbf{F}_{y_1 \theta^t} \phi_2 \\ \vdots \\ -\mathbf{F}_{y_1 \phi_{n_y}} \boldsymbol{\theta} - \mathbf{F}_{y_1 \theta^t} \phi_{n_y} \end{pmatrix}, \dots, \frac{\partial \mathbf{r}}{\partial f_{n_y+1}} = \frac{\partial \mathbf{r}}{\partial f_{u_1}} = \begin{pmatrix} -\mathbf{F}_{u_1 \phi_1} \boldsymbol{\theta} - \mathbf{F}_{u_1 \theta^t} \phi_1 \\ -\mathbf{F}_{u_1 \phi_2} \boldsymbol{\theta} - \mathbf{F}_{u_1 \theta^t} \phi_2 \\ \vdots \\ -\mathbf{F}_{u_1 \phi_{n_y}} \boldsymbol{\theta} - \mathbf{F}_{u_1 \theta^t} \phi_{n_y} \end{pmatrix}, \dots, \frac{\partial \mathbf{r}}{\partial f_{n_y+n_u+1}} = \frac{\partial \mathbf{r}}{\partial f_{\theta_1}} = \begin{pmatrix} -\phi_{1,1} \\ -\phi_{2,1} \\ \vdots \\ -\phi_{n_y,1} \end{pmatrix},$$

$$\frac{\partial \mathbf{r}}{\partial f_{n_f}} = \frac{\partial \mathbf{r}}{\partial f_{\theta_{n_\theta}}} = \begin{pmatrix} -\phi_{1,n_\theta} \\ -\phi_{2,n_\theta} \\ \vdots \\ -\phi_{n_y,n_\theta} \end{pmatrix}$$

Remark 7: Since coefficients of matrices $\mathbf{F}_{y\theta^t}$ and $\mathbf{F}_{u\theta^t}$ may depend on faults \mathbf{f} (see Remark 5) the sensitivity (18) as well.

Residual fault sensitivity (18) can be used to characterize the minimum detectable fault (see next section) and to enhance fault isolation as well as to allow fault estimation (see Section 5).

4.3 Minimum Detectable Fault

According to Gertler (1998), the *minimum detectable fault* corresponds to a fault that brings a residual to its threshold (“*triggering limit*”), assuming that no other faults and nuisance inputs are present. The minimum detectable fault was defined in Blesa *et al.* (2010) for single output LPV systems (i.e. $n_y=1$ in (1)). Here, it is extended to the MIMO systems (1) by considering that the residual (13), in presence of a single fault f , can be approximated by $\mathbf{r}(k) \approx \mathbf{s}_f(q^{-1})f(k)$ where $\mathbf{s}_f(q^{-1})$ is the vector that contains the residual fault sensitivity to the fault f and corresponds with a column of fault sensitivity matrix (18). Then, the minimum detectable fault can be computed as

$$\left| f_f^{\min}(k) \right| = \min \left(\left| f_{f:r_1}^{\min}(k) \right|, \dots, \left| f_{f:r_{n_y}}^{\min}(k) \right| \right) \quad (19)$$

where

$$\left| f_{f:r_i}^{\min}(k) \right| = \frac{\delta_{r_i}(k)}{\left| s_{f:i}(q^{-1}) \right|} \quad (20)$$

with

$$s_{f:i}(q^{-1}) = \frac{\partial r_i}{\partial f} \quad (21)$$

and,

$$\delta_{r_i}(k) = 2 \left\| \boldsymbol{\phi}_i(k) \mathbf{H} \right\|_1 + 2\sigma_i \quad (22)$$

is computed as according to Blesa *et al.* (2011).

Notice that the term $\delta_{r_i}(k)$ considers uncertainty in parameters. Moreover, Eq. (20) defines the minimum detectable fault using residual r_i . Therefore, the minimum detectable fault using the fault detection procedure presented in *Section 4.1* is the smallest of the minimum detectable faults of the n_y residuals according to (19).

5. FAULT ISOLATION AND ESTIMATION METHODOLOGY

5.1 Introduction

Fault isolation consists in identifying the faults affecting the system. Fault isolation could be carried out, as classically proposed in FDI books (Gertler, 1998)(Isermann, 2006), on the basis of fault signatures generated by the fault detection test (14) applied component-wise to each single residual

$$\phi_i(k) = \begin{cases} 0 & \text{if } 0 \in \Gamma_i(k) \\ 1 & \text{if } 0 \notin \Gamma_i(k) \end{cases} \quad (23)$$

producing an *observed fault signature* $\phi(k)$:

$$\phi(k) = (\phi_1(k), \phi_2(k), \dots, \phi_{n_p}(k)) \quad (24)$$

Then, the observed fault signature is supplied to the fault isolation module that has the knowledge about the binary relation between the considered fault hypothesis set $\mathbf{f}(k) = \{f_1(k), f_2(k), \dots, f_{n_f}(k)\}$ and the fault signal set $\phi(k)$. This relation is stored in the so called *theoretical binary fault signature matrix (FSM)*. An element $FSM_{i;j}$ of this matrix is equal to 1 if the fault hypothesis $f_j(k)$ is expected to affect the residual $r_i(k)$, that is, the related fault signal $\phi_i(k)$ is equal to 1 when this fault is affecting the monitored system. Otherwise, the element $FSM_{i;j}$ is zero-valued.

However, this basic fault detection and isolation scheme has the drawback that does not consider the MIMO nature of the residuals (13) when generating the observed fault signature (24) since each residual is evaluated independently of the others, while in fault detection (14) all residual components are evaluated altogether. Moreover, as discussed in (Meseguer *et al.*, 2010), the binarisation process used to generate the observed fault signature (24) causes a loss of useful information that can reduce fault isolability of the fault isolation algorithm. To address both issues, a fault isolation algorithm based on the residual fault sensitivity is proposed in the following.

5.2 Fault isolation and estimation algorithm

The information of the residual fault sensitivity matrix (18) can be used for isolation and estimation purposes extending the idea presented in Zhang and Jiang (2005) for parametric faults in single output systems. In this approach, the fault isolation and estimation is formulated as a *Variable-Length Sliding Window Blockwise Least Squares* parameter estimation. Considering that the fault vector is given by

$$\mathbf{f}(k) = \begin{cases} \mathbf{0}, & k < k_{fault} \\ \mathbf{f}_o, & k \geq k_{fault} \end{cases}$$

i.e., faults have appeared at instant k_{fault} and $\mathbf{f}_o \in \mathbb{R}^{n_f}$. Then, the problem of fault isolation and estimation implies solving *Problem 3*, for $k \geq k_{fault}$ once the fault has been detected.

Problem 3: “Fault isolation and estimation (multiple faults)”

$$\mathbf{f}_0(k) = \arg \min_{\mathbf{f}} \{J(\mathbf{f}, k)\}$$

subject to $J(\mathbf{f}, k) = \sum_{i=\max\{k_{fault}, k-\ell+1\}}^k \left\| \mathbf{r}^0(i) - \mathbf{S}(q^{-1}, \boldsymbol{\theta}^0(\mathbf{p}_i), \mathbf{f}) \mathbf{f} \right\|^2$

where

- $\mathbf{r}^0(k) = \mathbf{y}(k) - \hat{\mathbf{y}}^0(k)$
- ℓ is the time moving horizon where the fault is considered constant.

Remark 8: Notice that formulating the fault isolation problem in this way, the residual fault sensitivity (18) that depends on the fault (see *Remark 7*) can be used for fault isolation (estimation) even though the fault is unknown. Moreover, with this formulation the fault effect in the scheduling variable described in *Remark 5* can be taken into account in the fault isolation and estimation.

This non-linear optimization problem can be particularized for parametric faults (\mathbf{f}_θ) and single output systems ($n_y = 1$) since in this case: $\mathbf{S}(q^{-1}, \boldsymbol{\theta}^0(\mathbf{p}_i), \mathbf{f}) = \partial r^0 / \partial \mathbf{f}_\theta = \boldsymbol{\phi}(k)$ and the objective function of *Problem 3* can be formulated as follows

$$J(\mathbf{f}_\theta, k) = \sum_{i=\max\{k_{fault}, k-\ell+1\}}^k \left(r^0(i) - \boldsymbol{\phi}(i) \mathbf{f}_\theta \right)^2 \quad (25)$$

corresponding to a minimum least square parameter identification problem.

The role of the time moving horizon ℓ is to minimize the noise effects since the longer the moving horizon is, the smaller this effects will be. However, increasing the moving horizon will lead to slower fault isolation. Then, the window length has to be chosen as the minimum window that provides similar isolation and estimation results compared with longer windows. This has

been extensively discussed in Zhang and Jiang (2005), where the isolation and estimation approach proposed in this paper has been inspired.

Problem 3 can be simplified when single faults are considered since in this case the fault vector can be parameterized as follows

$$\mathbf{f}(k) = \begin{cases} (0 \ \cdots \ 0 \ \cdots \ 0)^t, & k < k_{fault} \\ f_o(0 \ \cdots \ 1 \ \cdots \ 0)^t, & k \geq k_{fault} \end{cases} \quad (26)$$

with $f_o \in \mathbb{R}$.

On the other hand, *Problem 3* can be simplified when single faults (26) are considered. Then, the problem of fault isolation and estimation implies solving *Algorithm 1*.

Algorithm 1: “Fault isolation and estimation (single faults)”

1: **for** $j=1, \dots, n_f$ **do**

2: $(J_j^{opt}(k), f_j^{opt}(k)) \leftarrow \min_f J_j(f, k)$

subject to $J_j(f, k) = \sum_{i=\max\{k_{fault}, k-\ell+1\}}^k \|\mathbf{r}^0(i) - \mathbf{s}_{-j}^0 f\|^2$

where

$-\mathbf{s}_{-j}^0 = \partial \mathbf{r}^0 / \partial f_j$ is the j^{th} column of $\mathbf{S}(q^{-1}, \boldsymbol{\theta}^0(\mathbf{p}_k), \mathbf{f})$

3: **endfor**

4: $I(k) = \arg \min_{j \in \{1, \dots, n_f\}} \{J_j^{opt}(k)\}$

5: $f_0(k) = f_{I(k)}^{opt}(k)$

Remark 9: *Algorithm 1* implies solving n_f multi-output least square error optimization problems as (25) for every n_f possible single faults. The most probable fault $I(k)$ is determined as the fault that gives the minimum function cost $J_j(f, k)$ after solving the set of least square error problems for the set of considered single faults.

Remark 10: A fault f_j will be isolable, from the other $n_f - 1$ faults using *Algorithm 1* when

$$J_j^{opt}(k) < J_i^{opt}(k) \quad \forall i \in \{1, \dots, n_f\} \quad i \neq j \quad \forall k \geq k_{fault} \quad (27)$$

Then, the minimum isolable fault f_j will be the one with the smallest size such that (27) is satisfied. This size depends on the minimum distance between s_{-j}^0 and the rest of the columns of $\mathbf{S}(q^{-1}, \boldsymbol{\theta}^0(\mathbf{p}_k), \mathbf{f})$: The bigger the minimum distance between columns the smaller minimum isolable fault will be. As a consequence, the fault isolation error rate will decrease when this distance increase.

6. APPLICATION CASE STUDY 1: PIECE OF WATER DISTRIBUTION NETWORK

6.1 Description of the system

The first application case study to test the proposed approach is focused on the leak detection and isolation problem in a piece of a water distribution network (see Fig. 2). This problem is particularly important in water distribution networks and currently is still a field of research (Pérez *et al.*, 2011). One of the main difficulties of using a model-based approach to address this problem is due to the behaviour of the network is described by a multivariable input/output system described by a set of non-linear equations that does not have explicit solution. The method proposed in this paper can be considered a novel approach to this problem with respect the current approaches existing in the literature. Here, just for illustration purposes, a small piece of a water distribution network is considered, but it could be easily extended to a real size network just proceeding with the proposed methodology. The considered piece is composed by the following elements: Three pipes with flows q_1 , q_2 and q_3 (in m^3/s) and two nodes with demands d_1 and d_2 (in m^3/s). Pressure sensors provides heads h_{r1} , h_{r2} , h_{n1} and h_{n2} (in m). Sensors that measure h_{r1} , h_{r2} are located in the inputs of the piece of the system while sensors that measure h_{n1} , h_{n2} are located in the two nodes. The possible faults are f_1 and f_2 that correspond to leaks located in the nodes.

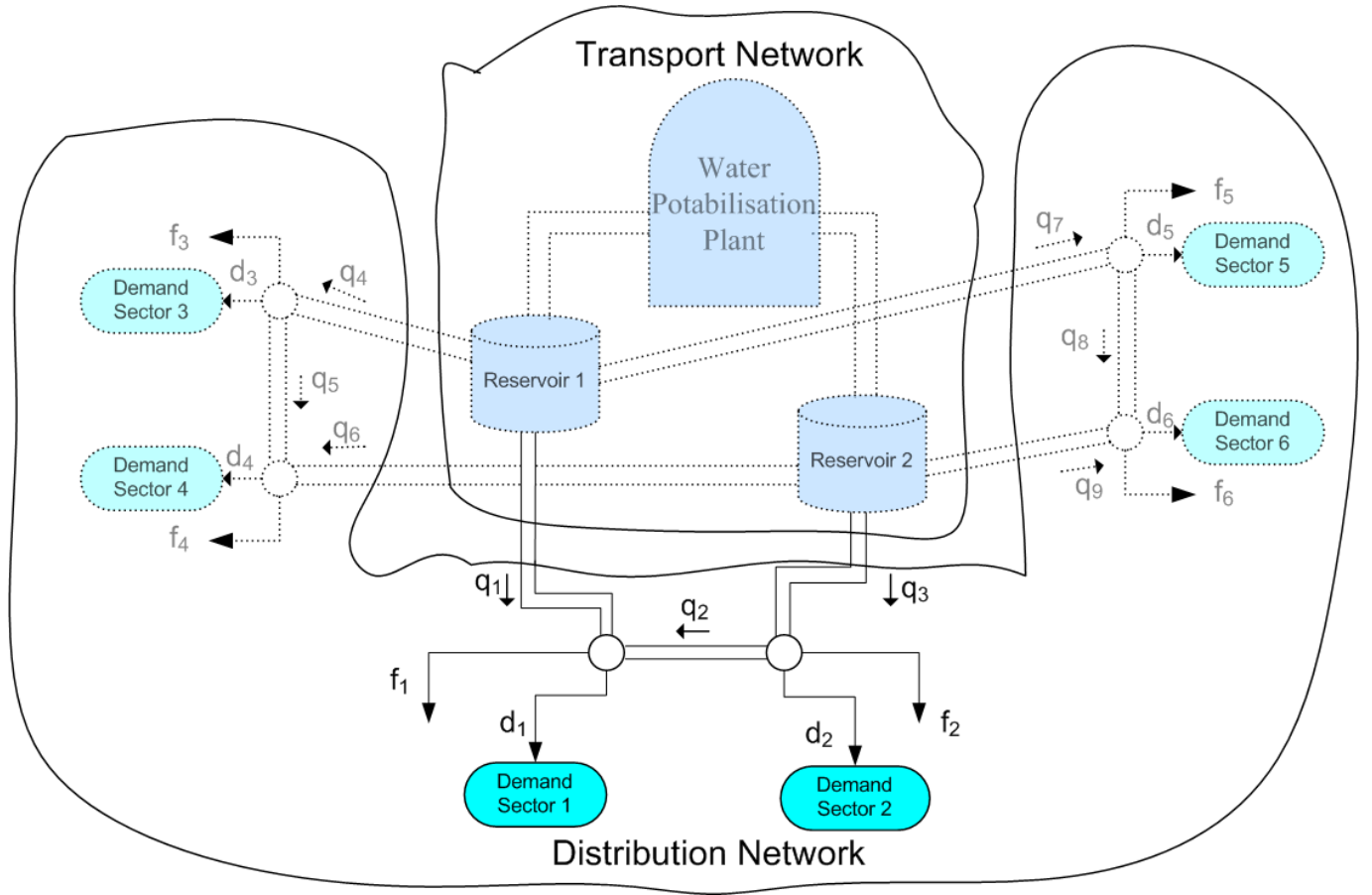


Figure 2. Piece of water distribution network proposed as case study

6.2 Water network distribution modelling

Considering the flow continuity condition in the two nodes included in this case study

$$q_1(k) + q_2(k) - d_1(k) - f_1(k) = 0 \quad (28)$$

$$q_3(k) - q_2(k) - d_2(k) - f_2(k) = 0 \quad (29)$$

and applying the Hazen-Williams (H-W) formula (Brdys and Ulanicki, 1994) to the pipe flows in (28) and (29), the following set of equations can be derived

$$\left(\frac{h_{r1}(k) - h_{n1}(k)}{R_1} \right)^{a-1} + \left(\frac{h_{n2}(k) - h_{n1}(k)}{R_2} \right)^{a-1} - d_1(k) - f_1(k) = 0 \quad (30)$$

$$\left(\frac{h_{r2}(k) - h_{n2}(k)}{R_3} \right)^{a-1} - \left(\frac{h_{n2}(k) - h_{n1}(k)}{R_2} \right)^{a-1} - d_2(k) - f_2(k) = 0 \quad (31)$$

where the pipe resistance coefficients R_1 , R_2 and R_3 in the H-W formula are given by $R = 1.2216 \cdot 10^{10} L / (C^a D^{4.87})$ where L is the pipe length (in m), D is the pipe diameter (in mm) and a is the flow exponent ($a = 1.852$). The length of the pipes is $L_1 = L_2 = 1000\text{m}$ and $L_3 = 2000\text{m}$ and their diameters are $D_1 = D_2 = D_3 = 200\text{mm}$.

This set of equations is non-linear since $a \neq 1$ and can not be solved analytically to obtain the node heads, but instead numerical methods should be used (Brdys and Ulanicki, 1994). This non-linearity also makes difficult to estimate the parameters of the network (as, e.g. the pipe resistances). For all these reasons, the non-linear model of the network is not very useful for FDI. But in this paper, it will be used as a virtual reality using the high-fidelity simulator EPANET.

In order to apply the proposed methodology, an LPV model for this network will be derived by means of the linearisation of the non-linear model (30) and (31), considering no fault is present, around a generic operating point characterised by the head measurements in nodes (h_{n1}^0 and h_{n2}^0)

$$\begin{pmatrix} \hat{h}_{n1}(k) \\ \hat{h}_{n2}(k) \end{pmatrix} = A_{hm}^{-1} \begin{pmatrix} d_1(k) \\ d_2(k) \end{pmatrix} + A_{hm}^{-1} \begin{pmatrix} F_1(h_{n1}^0(k), h_{n2}^0(k)) \\ F_1(h_{n1}^0(k), h_{n2}^0(k)) \end{pmatrix} + \begin{pmatrix} h_{n1}^0(k) \\ h_{n2}^0(k) \end{pmatrix} \quad (32)$$

where

$$A_{hm} = \begin{pmatrix} \frac{\left(\frac{h_{r1}(k) - h_{n1}^0(k)}{R_1}\right)^{\frac{1}{a}-1}}{aR_1} & \frac{\left(\frac{h_{n2}^0(k) - h_{n1}^0(k)}{R_2}\right)^{\frac{1}{a}-1}}{aR_2} & \frac{\left(\frac{h_{n2}^0(k) - h_{n1}^0(k)}{R_2}\right)^{\frac{1}{a}-1}}{aR_2} \\ \frac{\left(\frac{h_{n2}^0(k) - h_{n1}^0(k)}{R_2}\right)^{\frac{1}{a}-1}}{aR_2} & \frac{\left(\frac{h_{r2}(k) - h_{n2}^0(k)}{R_3}\right)^{\frac{1}{a}-1}}{aR_3} & \frac{\left(\frac{h_{n2}^0(k) - h_{n1}^0(k)}{R_2}\right)^{\frac{1}{a}-1}}{aR_2} \end{pmatrix}$$

and

$$\begin{aligned} F_1(h_{n1}^0(k), h_{n2}^0(k)) &= \left(\frac{h_{r1}(k) - h_{n1}^0(k)}{R_1}\right)^{a-1} + \left(\frac{h_{n2}^0(k) - h_{n1}^0(k)}{R_2}\right)^{a-1} - d_1(k) - f_1(k) \\ F_2(h_{n1}^0(k), h_{n2}^0(k)) &= \left(\frac{h_{r2}(k) - h_{n2}^0(k)}{R_3}\right)^{a-1} - \left(\frac{h_{n2}^0(k) - h_{n1}^0(k)}{R_2}\right)^{a-1} - d_2(k) - f_2(k) \end{aligned}$$

Notice that parameters vary with node heads. But, according to (30) and (31), the node heads are fixed by the demands in a complex way. For this reason, the LPV model (32) can be approximated as follows

$$\begin{pmatrix} \hat{h}_{n1}(k) \\ \hat{h}_{n2}(k) \end{pmatrix} = \begin{pmatrix} a_{1,1}(d_1(k), d_2(k)) & a_{1,2}(d_1(k), d_2(k)) \\ a_{2,1}(d_1(k), d_2(k)) & a_{2,2}(d_1(k), d_2(k)) \end{pmatrix} \begin{pmatrix} d_1(k) \\ d_2(k) \end{pmatrix} + \begin{pmatrix} a_{1,3}(d_1(k), d_2(k)) \\ a_{2,3}(d_1(k), d_2(k)) \end{pmatrix} \quad (33)$$

where $a_{1,2}(d_1(k), d_2(k)) = a_{2,1}(d_1(k), d_2(k))$ and the model parameter dependence with the demand can be approximated by an experimental relation as follows

$$a_{i,j}(\mathbf{p}_k) = \alpha_{i,j}d_1(k) + \beta_{i,j}d_2(k) + \gamma_{i,j} \quad i = 1, 2 \text{ and } j = 1, 2 \quad (34)$$

where the parameters $\alpha_{i,j}$, $\beta_{i,j}$ and $\gamma_{i,j}$ are estimated using measurements and identification algorithms.

Finally, considering bounded additive noise in the pressure sensors, LPV model (33) can be rewritten in regressor form (1) as follows

$$\mathbf{y}(k) = \begin{pmatrix} h_{n1}(k) \\ h_{n2}(k) \end{pmatrix}, \mathbf{\Phi}(k) = \begin{pmatrix} d_1(k) & d_2(k) & 0 & 1 & 0 \\ 0 & d_1(k) & d_2(k) & 0 & 1 \end{pmatrix}, \boldsymbol{\theta}(\mathbf{p}_k) = (a_{1,1}(\mathbf{p}_k) \ a_{1,2}(\mathbf{p}_k) \ a_{2,2}(\mathbf{p}_k) \ a_{1,3}(\mathbf{p}_k) \ a_{2,3}(\mathbf{p}_k))^t \quad (35)$$

where $\mathbf{p}_k = \begin{pmatrix} d_1(k) \\ d_2(k) \end{pmatrix}$, $\mathbf{e}(k) = \begin{pmatrix} e_1(k) \\ e_2(k) \end{pmatrix}$

In Annex 2, the procedure followed to apply the proposed identification and fault diagnosis approach is summarised in an algorithmic way.

6.2 Identification

The parameter identification of model (35), considering the parameter set described by the zonotope (2), has been carried out in two steps: first estimation of nominal parameters and second estimation of its uncertainty defined by \mathbf{H} .

For the nominal parameter estimation, the LPV parameter estimation algorithm proposed by Bamieh and Giarré (2002) has been applied to a set of head/demand data recorded in the network in a non-leak scenario (fault free scenario) considering noise bounds given by sensors accuracy. The parameters $\alpha_{i,j}$, $\beta_{i,j}$ and $\gamma_{i,j}$ in Eq. (34) obtained are showed in Table 1.

$\alpha_{1,1}$	0.0039	$\alpha_{2,1}$	-0.0023
$\beta_{1,1}$	-1.11	$\beta_{2,1}$	-0.0046
$\gamma_{1,1}$	1.11	$\gamma_{2,1}$	1.77
$\alpha_{1,2}$	-0.0023	$\alpha_{2,2}$	-1.21
$\beta_{1,2}$	-0.0046	$\beta_{2,2}$	-0.0016
$\gamma_{1,2}$	1.77	$\gamma_{2,2}$	3.01
$\alpha_{1,3}$	1.11	$\alpha_{2,3}$	0.633
$\beta_{1,3}$	3.77	$\beta_{2,3}$	3.01
$\gamma_{1,3}$	3.89	$\gamma_{2,3}$	2.94

Table 1. Coefficients of nominal LPV parameters (34)

After the nominal LPV model has been estimated, parametric modelling uncertainty has been obtained solving *Problem 1*, considering that there are not dependencies between parameters and the same uncertainty weight is used in every parameter, through the following parameterization

$$a_{i,j}(\mathbf{p}_k) \in [a_{i,j}^0(\mathbf{p}_k) - \lambda, a_{i,j}^0(\mathbf{p}_k) + \lambda] \quad i = 1, 2 \text{ and } j = 1, 2 \quad (36)$$

where $a_{i,j}^0(\mathbf{p}_k)$ are the nominal parameter given by Equation (34) and coefficients of Table 1. Then, \mathbf{H} in (2) is $\mathbf{H} = \lambda \mathbf{H}_0$ with $\mathbf{H}_0 = \mathbf{I}$. Using the same non-faulty data set used for the nominal identification, uncertain parameter λ is determined by solving *Problem 1* and it results in $\lambda = 2.05 \cdot 10^{-5}$.

Once the model has been calibrated, fault detection test (*Problem 2*) has been applied to different non-faulty scenarios in order to validate the model.

6.3 Fault Detection, Isolation and Estimation

The faults to be detected, isolated and estimated correspond to leaks in nodes 1 and 2. These faults can be interpreted as unknown changes in demands d_1 and d_2 and are denoted as: $d_{1f} = d_1 + f_1$ and $d_{2f} = d_2 + f_2$, respectively. Only single faults have been considered.

Combining (33) with (13), residuals are obtained. Then, the residual fault sensitivity transfer function matrix (18) is

$$\mathbf{S} = \begin{pmatrix} S_{1;1} & S_{1;2} \\ S_{2;1} & S_{2;2} \end{pmatrix} \quad (37)$$

with

$$S_{1;1} = a_{1;1}(d_{1f}, d_2) + d_{1f} \alpha_{1;1} + d_2 \alpha_{1;2} + \alpha_{1;3}$$

$$S_{1;2} = a_{1;2}(d_1, d_{2f}) + d_1 \alpha_{1;2} + d_{2f} \alpha_{2;2} + \alpha_{2;3}$$

$$S_{2;1} = a_{1;2}(d_{1f}, d_2) + d_{1f} \beta_{1;1} + d_2 \beta_{1;2} + \beta_{1;3}$$

$$S_{2;2} = a_{2;2}(d_1, d_{2f}) + d_1 \beta_{1;2} + d_{2f} \beta_{2;2} + \beta_{2;3}$$

On the other hand, the theoretical binary fault signature matrix *FSM* is given by

	f_1	f_2
r_1	1	1
r_2	1	1

Table 2: Theoretical binary fault signature matrix of the two different considered faults

From Table 2, it can be noticed that the two leaks can not be isolated using the classic fault isolation approach (recalled in *Section 5.1*) but are distinguishable using the residual fault sensitivity transfer function matrix (37) since $\text{rank}(\mathbf{S})=2$.

6.4 Fault scenarios

In the following, two different fault scenarios have been simulated and the results of the fault detection, isolation and estimation procedure are presented.

Fault scenario 1: “Leak $f_l=0.5$ l/s is present in the node 1 at time $1.7 \cdot 10^5$ s.”. Fig. 3(a) shows the components of the nominal MIMO residuals in the leak scenario 1. These residuals are considered as the difference between the real and predicted head measurements using the LPV model (33) with nominal parameters (34).

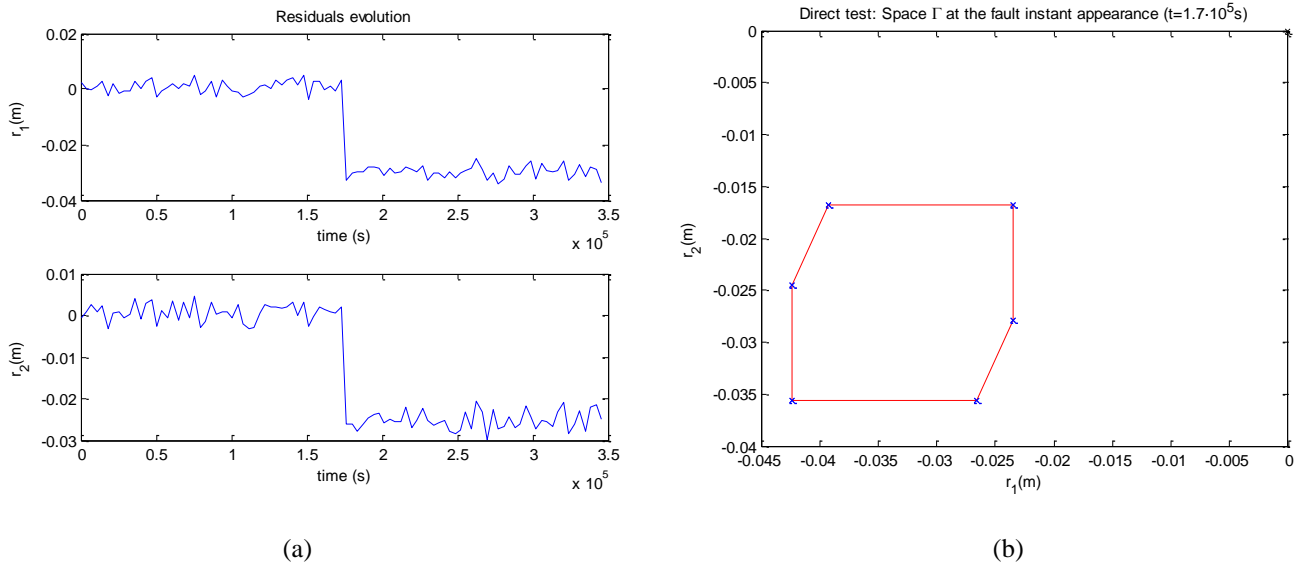


Figure 3. (a) Residuals evolution in fault scenario 1. (b) Fault test in fault scenario 1.

Fig. 3 (b) shows the set Γ , defined by (15), at the fault appearance instant. Notice that since the set Γ does not contain the point $(0,0)$, the leak is detected according to (14) and leading to non feasibility of *Problem 2*.

After the fault has been detected at time $1.7 \cdot 10^5$ s, it should be isolated and estimated. Fig. 4(a) shows the minimum of optimisation cost functions ($J(f_1)$ and $J(f_2)$) defined in *Algorithm 1*. A window length $\ell = 20$ has been chosen as the minimum window that provides similar isolation and estimation results compared with longer windows.

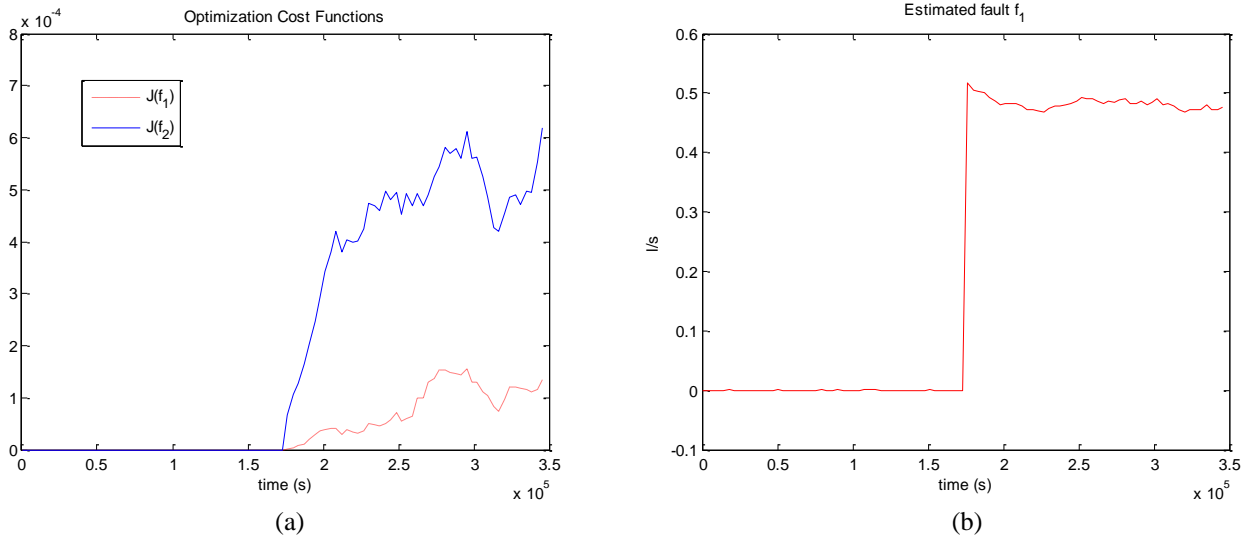


Figure 4. (a) Optimization cost functions in leak scenario 1. (b) Fault estimation.

As $J(f_1)$ is smaller than $J(f_2) \forall k \geq 1.7 \cdot 10^5 s$, then a leak is located in node 1. Thus, the leak magnitude f_1 , presented in Fig. 4 (b), is obtained as one that provides the smallest minimum of $J(f_1)$ when solving *Algorithm 1*.

Fault scenario 2: "Leak $f_2=0.6 l/s$ is present in the node 2 at time $1.7 \cdot 10^5 s$ ". Fig. 5 (a) shows the components of the nominal MIMO residuals in the leak scenario 2.

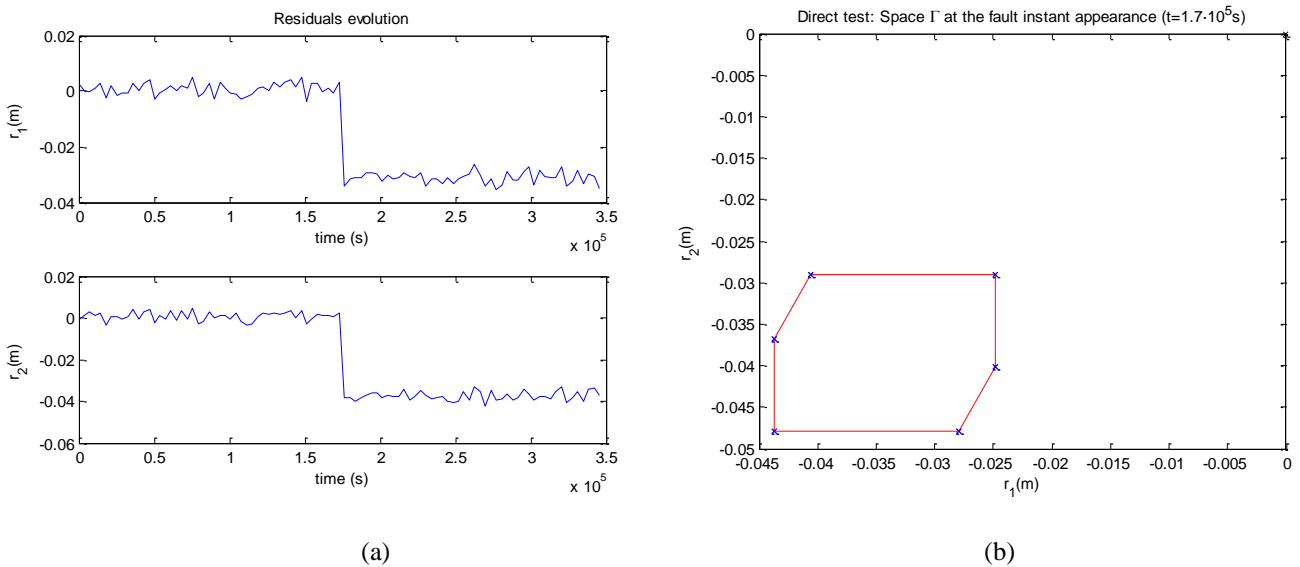


Figure 5. (a) Residuals evolution in fault scenario 2. (b) Fault test in fault scenario 2.

As in the previous scenario, after the fault has been detected at time $1.7 \cdot 10^5$ s, it should be isolated and estimated. Fig. 6(a) shows the minimum of optimisation cost functions ($J(f_1)$ and $J(f_2)$) defined in *Algorithm 1* with the same window length used in fault scenario 1.

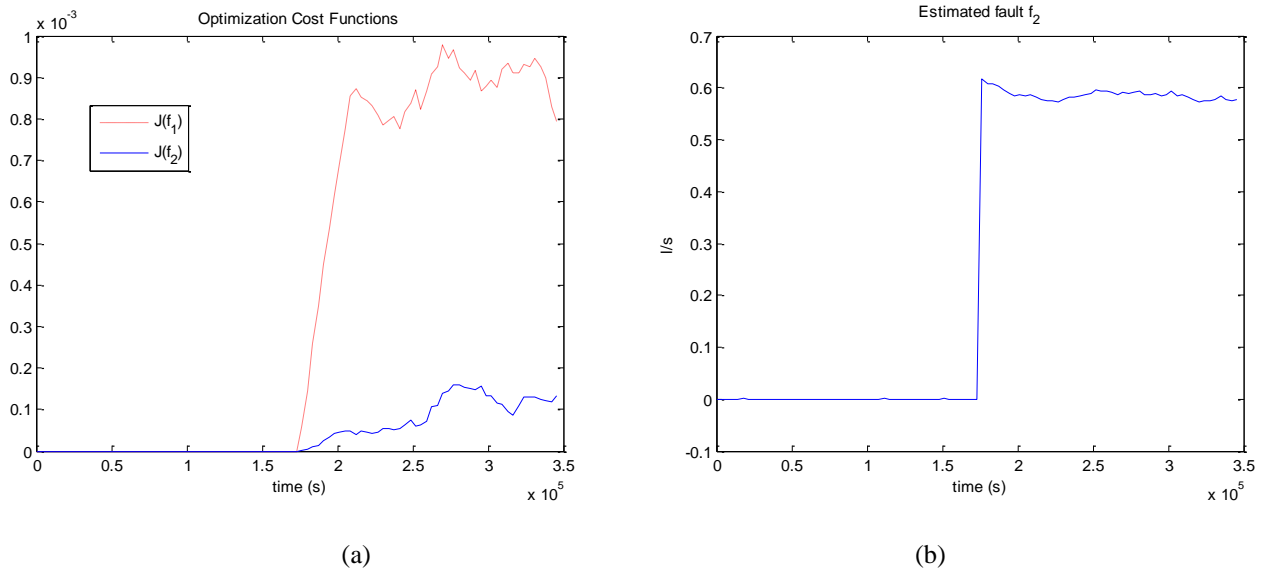


Figure 6. (a) Optimisation cost functions in leak scenario 2. (b) Fault estimation. Both figures begin in the fault time detection of fault scenario 2 ($t=1.7 \cdot 10^5$ s)

As $J(f_2)$ is smaller than $J(f_1) \forall k \geq 1.7 \cdot 10^5$ s, then a leak is located in node 1. Thus, the leak magnitude f_1 , presented in Fig. 6(b), is obtained as the minimiser $J(f_2)$ of that results from solving *Algorithm 1*.

Figure 5 (b) shows the set Γ , defined by (15), at the fault instant appearance. Notice that since the set Γ does not contain the point (0,0), the leak is detected according to (14).

7. CASE STUDY 2: FOUR TANK SYSTEM

7.1 Description of the system

A quadruple-tank process, proposed by Johansson (2000), is used as second case study to illustrate the effectiveness of the fault diagnosis method proposed in this paper. This example differs from the previous one that model equations are now dynamic. A schematic diagram of the quadruple-tank system is shown in Fig. 7. The inputs are v_1 and v_2 (input voltages to the pumps) and the outputs are the tank levels h_1 , h_2 , h_3 and h_4 .

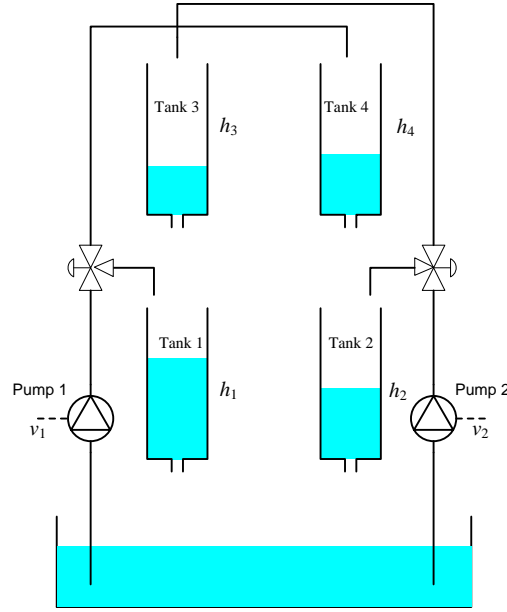


Figure 7: Quadruple-tank process.

The equations that describe the system presented in (Johansson, 2000) discretised by means of the Euler method with sampling time $\Delta t = 1s$ are

$$\begin{aligned}
 h_1(k) &= \left(1 - \frac{a_1}{A_1} \sqrt{\frac{2g}{h_1(k-1)}}\right) h_1(k-1) + \frac{a_3}{A_1} \sqrt{\frac{2g}{h_3(k-1)}} h_3(k-1) + \frac{\gamma_1 k_1}{A_1} v_1(k-1) + e_1(k) \\
 h_2(k) &= \left(1 - \frac{a_2}{A_2} \sqrt{\frac{2g}{h_2(k-1)}}\right) h_2(k-1) + \frac{a_4}{A_2} \sqrt{\frac{2g}{h_4(k-1)}} h_4(k-1) + \frac{\gamma_2 k_2}{A_2} v_2(k-1) + e_2(k) \\
 h_3(k) &= \left(1 - \frac{a_3}{A_3} \sqrt{\frac{2g}{h_3(k-1)}}\right) h_3(k-1) + \frac{(1-\gamma_2)k_2}{A_3} v_2(k-1) + e_3(k) \\
 h_4(k) &= \left(1 - \frac{a_4}{A_4} \sqrt{\frac{2g}{h_4(k-1)}}\right) h_4(k-1) + \frac{(1-\gamma_1)k_1}{A_4} v_1(k-1) + e_4(k)
 \end{aligned} \tag{38}$$

where $a_1 = a_3 = 0.071cm^2$, $A_1 = A_3 = 28cm^2$, $\gamma_1 = 0.7$, $k_1 = 3.33cm^3/Vs$, $a_2 = a_4 = 0.057cm^2$, $A_2 = A_4 = 32cm^2$, $\gamma_2 = 0.6$, $k_2 = 3.35cm^3/Vs$, $g = 981cm/s^2$ are the model parameters. $e_i(k)$, $i = 1, \dots, 4$ are the additive errors (including sensor and discretisation errors) that are assumed to be bounded. The bounds are $\sigma_i = 0.05cm$, $i = 1, \dots, 4$.

The non-linear model (38) can be expressed in quasi-LPV form (Shamma and Cloutier, 1993) by using the approach based on embedding the non-linearities inside the LPV parameters as proposed by (Kwiatkowski *et al.*, 2006). Following this procedure model (38) can be expressed as in (1) through the following parameterisation

$$\mathbf{y}(k) = (h_1(k) \ h_2(k) \ h_3(k) \ h_4(k))^t, \Phi(k) = (\Phi_1(k) \ \Phi_2(k)), \theta(\mathbf{p}_k) = \begin{pmatrix} \theta_1(\mathbf{p}_k) \\ \theta_2 \end{pmatrix} \tag{39}$$

$$\mathbf{e}(k) = (e_1(k) \ e_2(k) \ e_3(k) \ e_4(k))^t \tag{40}$$

with

$$\Phi_1(k) = \begin{pmatrix} h_1(k-1) & h_3(k-1) & 0 & 0 & 0 & 0 \\ 0 & 0 & h_2(k-1) & h_4(k-1) & 0 & 0 \\ 0 & 0 & 0 & 0 & h_3(k-1) & 0 \\ 0 & 0 & 0 & 0 & 0 & h_4(k-1) \end{pmatrix}, \quad \Phi_2(k) = \begin{pmatrix} v_1(k-1) & 0 & 0 & 0 \\ 0 & v_2(k-1) & 0 & 0 \\ 0 & 0 & v_2(k-1) & 0 \\ 0 & 0 & 0 & v_1(k-1) \end{pmatrix} \quad (41)$$

$$\theta_1(\mathbf{p}_k) = (a_{1,1}(\mathbf{p}_k) \ a_{1,3}(\mathbf{p}_k) \ a_{2,2}(\mathbf{p}_k) \ a_{2,4}(\mathbf{p}_k) \ a_{3,3}(\mathbf{p}_k) \ a_{4,4}(\mathbf{p}_k))^t, \quad \theta_2 = (b_{1,1} \ b_{2,2} \ b_{3,1} \ b_{4,2})^t \quad (42)$$

$$\mathbf{p}_k = (h_1(k-1) \ h_2(k-1) \ h_3(k-1) \ h_4(k-1))^t \quad (43)$$

where

$$a_{i,i}(\mathbf{p}_k) = 1 - \frac{a_i \sqrt{2g}}{A_i} g_i(\mathbf{p}_k), \quad i = 1, \dots, 4, \quad a_{1,3}(\mathbf{p}_k) = \frac{a_3 \sqrt{2g}}{A_1} g_3(\mathbf{p}_k) \quad \text{and} \quad a_{2,4}(\mathbf{p}_k) = \frac{a_4 \sqrt{2g}}{A_2} g_4(\mathbf{p}_k) \quad (44)$$

$$b_{1,1} = \frac{\gamma_1 k_1}{A_1}, \quad b_{2,2} = \frac{\gamma_2 k_2}{A_2}, \quad b_{3,1} = \frac{(1-\gamma_2)k_2}{A_3}, \quad b_{4,2} = \frac{(1-\gamma_1)k_1}{A_4} \quad (45)$$

Additionally to additive noise, there is uncertainty in parameters $a_{j,i}$ because their value is adapted through the scheduling functions

$$g_i^0(\mathbf{p}_k) = \frac{1}{\sqrt{h_i(k-1)}} \quad i = 1, \dots, 4 \quad (46)$$

that depend on the measured variables (43) that are contaminated with noise leading to consider its effect as follows.

$$g_i(\mathbf{p}_k) = g_i^0(\mathbf{p}_k) + \Delta g_i(k) \quad i = 1, \dots, 4 \quad (47)$$

Then, the LPV vector parameter $\theta(\mathbf{p}_k)$ can be expressed as

$$\theta(\mathbf{p}_k) = \begin{pmatrix} \theta_1^0(\mathbf{p}_k) \\ \theta_2 \end{pmatrix} + \begin{pmatrix} \Delta \theta_1(k) \\ 0 \end{pmatrix} \quad (48)$$

with nominal parameters

$$\theta_1^0(\mathbf{p}_k) = (a_{1,1}^0(\mathbf{p}_k) \ a_{1,3}^0(\mathbf{p}_k) \ a_{2,2}^0(\mathbf{p}_k) \ a_{2,4}^0(\mathbf{p}_k) \ a_{3,3}^0(\mathbf{p}_k) \ a_{4,4}^0(\mathbf{p}_k))^t \quad (49)$$

where $a_{j,i}^0(\mathbf{p}_k)$ are obtained with (41) considering $g_i(\mathbf{p}_k) = g_i^0(\mathbf{p}_k)$ and uncertainty

$$\Delta \theta_1(k) = \sqrt{2g} \begin{pmatrix} -\frac{a_1}{A_1} \Delta g_1(k) & \frac{a_3}{A_1} \Delta g_3(k) & -\frac{a_2}{A_2} \Delta g_2(k) & \frac{a_4}{A_2} \Delta g_4(k) & -\frac{a_3}{A_3} \Delta g_3(k) & -\frac{a_4}{A_4} \Delta g_4(k) \end{pmatrix}^t \quad (50)$$

where

$$a_{i,i}^0 = 1 - \frac{a_i \sqrt{2g}}{A_i} g_i^0(\mathbf{p}_k), \quad i = 1, \dots, 4, \quad a_{1,3}^0 = \frac{a_3 \sqrt{2g}}{A_1} g_3^0(\mathbf{p}_k) \quad \text{and} \quad a_{2,4}^0 = \frac{a_4 \sqrt{2g}}{A_2} g_4^0(\mathbf{p}_k) \quad (51)$$

Parametric uncertainty can be expressed using a zonotope, as in (2), in the following way

$$\Delta\theta_1(k) \in \mathbf{H}\mathbb{B}^n \quad (52)$$

As in the previous application example, the procedure followed to apply the proposed identification and fault diagnosis approach is summarised in *Annex 2*,

7.2 Identification

Nominal parameters (49) have been obtained by the physical modelling of the system that leads to (51). On the other hand, in the following it is shown how the parameter uncertainty (52) has been estimated..

In order to apply identification techniques presented in *Section 3*, input/output data is recorded in a fault free scenario applying a pseudorandom binary sequence (PRBS's) in the pump inputs such that all the operation points ($v_1 \in [2.4, 3.8]$ V and $v_2 \in [2.3, 3.5]$ V) are swept (Fig. 8).

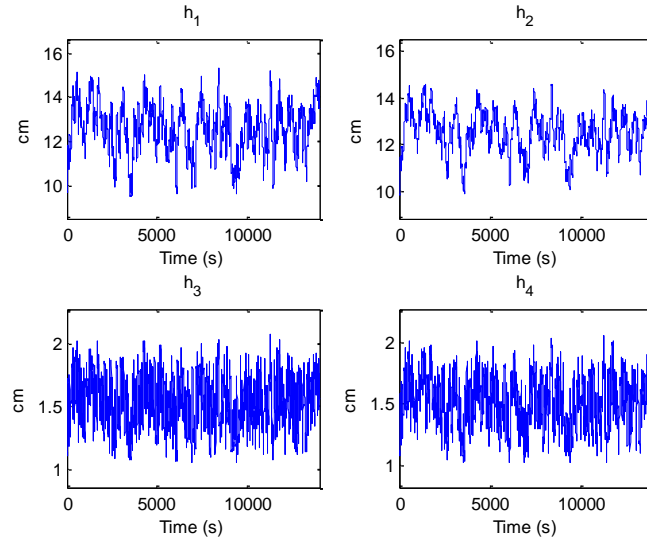


Figure 8: Fault free data using for parameter and uncertainty estimation (14000 samples)

The following parameterisation of matrix \mathbf{H} in (52), that takes into account physical relations in parametric uncertainties described in (50), has been used

$$\mathbf{H} = \mathbf{H}_t \mathbf{H}_g \quad (53)$$

with

$$\mathbf{H}_t = \sqrt{2g} \begin{pmatrix} \frac{-a_1}{A_1} & 0 & 0 & 0 & 0 & 0 \\ 0 & 0 & \frac{-a_2}{A_2} & 0 & 0 & 0 \\ 0 & \frac{a_3}{A_1} & 0 & 0 & \frac{-a_3}{A_3} & 0 \\ 0 & 0 & 0 & \frac{a_4}{A_2} & 0 & \frac{-a_4}{A_4} \end{pmatrix}^t \quad (54)$$

and $\mathbf{H}_g \in \mathbb{R}^{4 \times n}$ is the matrix to be identified that defines the zonotope that bounds parameters $\Delta \mathbf{g}(k)$, that is

$$\Delta \mathbf{g}(k) = \begin{pmatrix} \Delta g_1(k) \\ \Delta g_2(k) \\ \Delta g_3(k) \\ \Delta g_4(k) \end{pmatrix} \in \mathbf{H}_g \mathbb{B}^n \quad (55)$$

The uncertainty (52) of parameters (48) can be viewed as a linear transformation of $\Delta \mathbf{g}(k)$

$$\Delta \boldsymbol{\theta}(k) = \mathbf{H}_t \Delta \mathbf{g}(k) \quad (56)$$

The procedure of identification and fault detection presented in *Section 3* and *4*, respectively, can be carried out considering that $\hat{\Gamma}(k)$ in (9) can be parameterised as follows

$$\hat{\Gamma}(k) = (\boldsymbol{\Phi}_g(k) \mathbf{H}_g \quad \mathbf{E}) \mathbb{B}^{n+n}, \quad (57)$$

with

$$\boldsymbol{\Phi}_g(k) = \boldsymbol{\Phi}_1(k) \mathbf{H}_t = \sqrt{2g} \begin{pmatrix} \frac{-a_1}{A_1} h_1(k-1) & 0 & \frac{a_3}{A_1} h_3(k-1) & 0 \\ 0 & \frac{-a_2}{A_2} h_2(k-1) & 0 & \frac{a_4}{A_2} h_4(k-1) \\ 0 & 0 & \frac{-a_3}{A_3} h_3(k-1) & 0 \\ 0 & 0 & 0 & \frac{-a_4}{A_4} h_4(k-1) \end{pmatrix} \quad (58)$$

Let us consider $\mathbf{H}_g = \lambda \mathbf{H}_0$, with

$$\mathbf{H}_0 = -10^{-2} \begin{pmatrix} 0.93 & 0 & 0 & 0 \\ 0 & 0.77 & 0 & 0 \\ 1.3 & 0 & 8.4 & 0 \\ 0 & 1.22 & 0 & 8.74 \end{pmatrix} \quad (59)$$

estimated as it is described in *Annex 1* by dividing the data in 4 different directions. Fig. 9 shows the $\Delta g_1 - \Delta g_3$ and $\Delta g_2 - \Delta g_4$ projections of the zonotope $\mathbf{H}_0 \mathbb{B}^n$ and the 8 support polytopes ($\Delta \boldsymbol{\Theta}^j$ and $\Delta \bar{\boldsymbol{\Theta}}^j$ $j=1, \dots, 4$) used to compute \mathbf{H}_0 according to *Annex 1*.

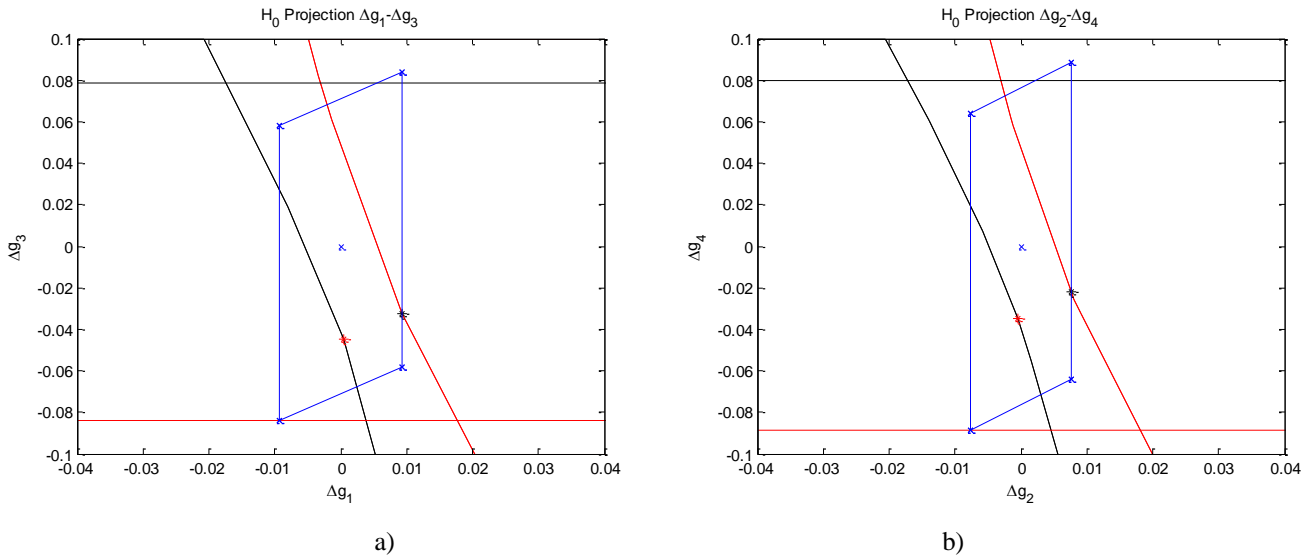


Figure 9: a) $\Delta g_1 - \Delta g_3$ and b) $\Delta g_2 - \Delta g_4$ projections of the zonotope $\mathbf{H}_0 \mathbb{B}^n$ (blue) and support polytopes (red and black).

Once \mathbf{H}_0 has been calculated, with the additive error bounds and nominal parameters obtained by the physical knowledge of the system, λ is computed solving *Problem 1* being equal to 0.762.

Once the model has been calibrated, fault detection test (*Problem 2*) has been applied to different non-faulty scenarios in order to validate the model.

7.3 Fault detection, isolation and estimation

In order to illustrate the fault detection, isolation and estimation procedure described in *Sections 4* and *5* (and presented in Fig. 1), in several fault scenarios, two different kinds of faults have been considered: additive faults (in input and output sensors: f_u and f_y) and multiplicative faults (in parameters: f_θ). The fault scenarios are created by introducing faults when the system is working in the operation range presented in Fig 10.

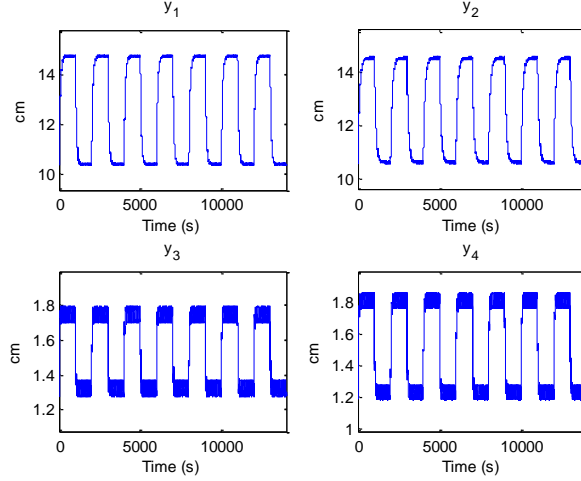


Figure 10: No faulty scenario data

In particular, the set of considered faults and their type is listed in the following:

Additive

- Input sensor faults $f_u : f_{v_1}$ and f_{v_2}
- output sensor faults $f_y : f_{h_1}, f_{h_2}, f_{h_3}$ and f_{h_4}

Multiplicative

- Component faults: $f_{a_1}, f_{a_2}, f_{a_3}, f_{a_4}, f_{\gamma_1}$ and f_{γ_2}

Only single faults have been considered.

Fault isolation and estimation method presented in *Section 5* is based on the fault sensitivity transfer function matrix (18). In our case study, with 4 residuals and 12 possible different faults to be detected, the matrix $\mathbf{S}(q^{-1}, \boldsymbol{\theta}(\mathbf{p}_k), \mathbf{f})$ of dimension (4×12) is

$$\mathbf{S}(q^{-1}, \boldsymbol{\theta}(\mathbf{p}_k), \mathbf{f}) = \begin{pmatrix} S_{1;1} & 0 & S_{1;3} & 0 & S_{1;5} & 0 & S_{1;7} & 0 & S_{1;9} & 0 & S_{1;11} & 0 \\ 0 & S_{2;2} & 0 & S_{2;4} & 0 & S_{2;6} & 0 & S_{2;8} & 0 & S_{2;10} & 0 & S_{2;12} \\ 0 & 0 & S_{3;3} & 0 & 0 & S_{3;6} & 0 & 0 & S_{3;9} & 0 & 0 & S_{3;12} \\ 0 & 0 & 0 & S_{4;4} & S_{4;5} & 0 & 0 & 0 & 0 & S_{4;10} & S_{4;11} & 0 \end{pmatrix} \quad (60)$$

On the other hand, the theoretical binary fault signature matrix *FSM* signature is given by

	f_{h_1}	f_{h_2}	f_{h_3}	f_{h_4}	f_{v_1}	f_{v_2}	f_{a_1}	f_{a_2}	f_{a_3}	f_{a_4}	f_{γ_1}	f_{γ_2}
r_1	1	0	1	0	1	0	1	0	1	0	1	0
r_2	0	1	0	1	0	1	0	1	0	1	0	1
r_3	0	0	1	0	0	1	0	0	1	0	0	1
r_4	0	0	0	1	1	0	0	0	0	1	1	0

Table 3: Theoretical binary fault signature matrix of the different considered faults

From Table 3, it can be noticed that there are some faults that can not be isolated with the binary fault signature matrix, even considering single faults. For example, the fault signature corresponding to the additive fault $f_{h_1} = (1 \ 0 \ 0 \ 0)^t$ is the same than the fault signature of the multiplicative fault $f_{a_1} = (1 \ 0 \ 0 \ 0)^t$. Therefore, they are not distinguishable. Whereas using the fault sensitivity matrix (60), the effect of both faults is $(S_{1;1} \ 0 \ 0 \ 0)^t$ and $f_{a_1} = (S_{1;7} \ 0 \ 0 \ 0)^t$, respectively, with

$$S_{1;1} = 1 \text{ and } S_{1;7} = \frac{\sqrt{2g(y_1(k-1) - f_{y_1}q^{-1})}}{A_1}. \text{ Thus, the two faults are distinguishable using the residual fault sensitivity (60).}$$

7.4 Faults scenarios

In the following, two different fault scenarios have been simulated and the results of the fault detection, isolation and estimation procedure are presented.

Fault scenario 1: “Sensor additive fault: $f_{h_1} = 0.8cm$ at $t=9500s$ ”

Figures 11a) and b) show the result of the detection test in this fault scenario. The fault is detected at the appearance time ($t=9500s$). At this time, the residual admissible space Γ does not contain the origin in the $r_1 - r_3$ projection. Thus, condition (14) is not fulfilled and derives in the non feasibility of *Problem 2* what proves the existence of a fault.

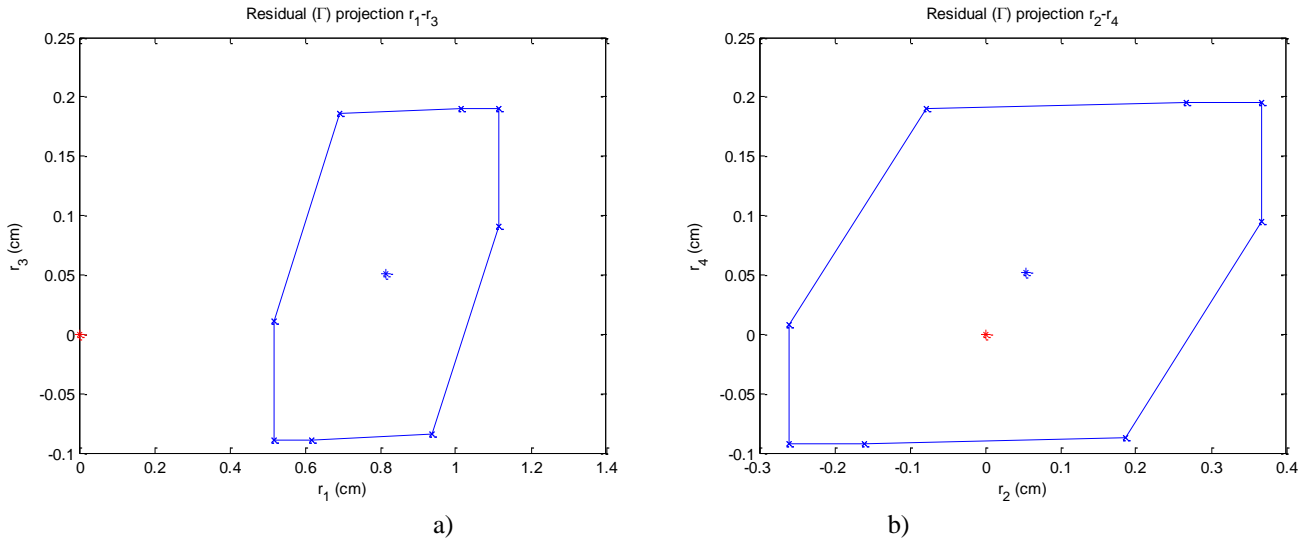


Figure 11: Residual admissible space Γ projections a) $r_1 - r_3$ and b) $r_2 - r_4$, at the fault time detection ($t=9500s$) in fault scenario 1.

After the fault has been detected, the fault isolation and estimation procedure is activated and *Algorithm 1* is solved considering the 12 possible different faults and using residual fault sensitivity (60). A window length $\ell = 20$ has been chosen as the minimum window that provides similar isolation and estimation results compared with longer windows.

Fig. 12 a) shows the evolution of the inverse of the optimisation cost function for different considered faults, obtained solving *Algorithm 1* from the fault detection time ($t=9500s$). As the objective function (J) corresponding to f_{h_1} is smaller than the objective function corresponding to the other faults considered, the fault isolation algorithm determines that the fault is an additive fault in output sensor h_1 . The fault magnitude estimation corresponding to f_{h_1} , determined also as result of the application of *Algorithm 1*, is presented in Fig. 12 b).

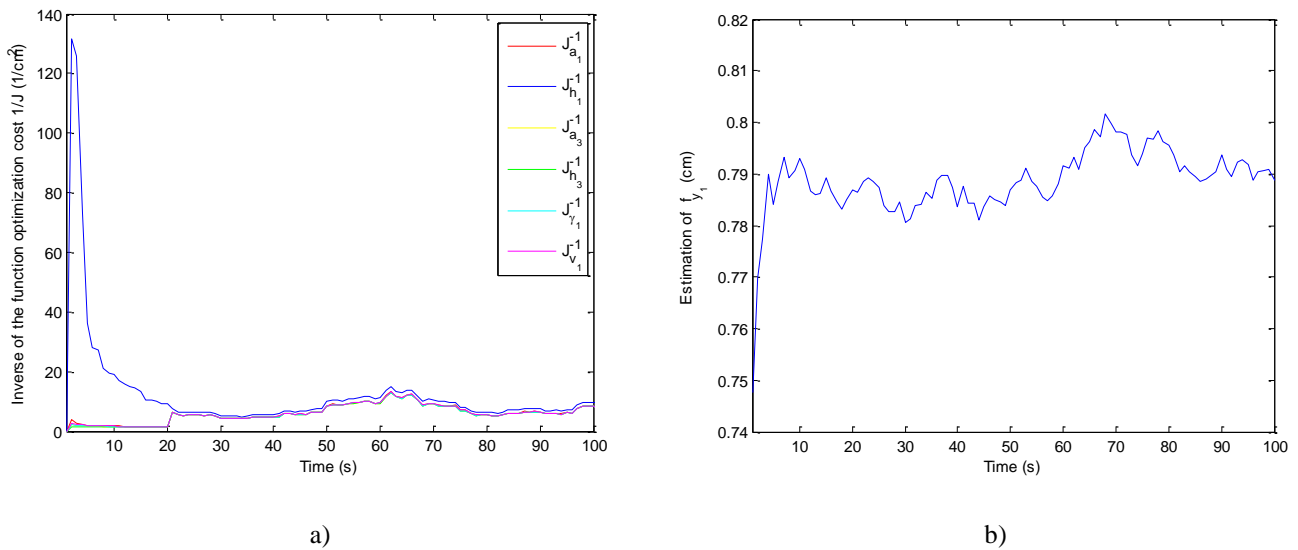


Figure 12: a) Inverse of optimisation cost function (J^{-1}) of different faults and b) fault estimation of f_{h_1} . Both figures begin in the fault time detection of fault scenario 1 ($t=9500s$).

Fault scenario 2: “Multiplicative fault: $f_{a_1} = 0.035\text{cm}^2$ at $t=8800\text{s}$ ”

In this case, the fault is detected at $t=8809\text{s}$, that is 9 seconds after the fault time appearance. Figures 13a) and b) show the result of the detection test at the detection time. It can be noticed in the $r_1 - r_3$ projection that since the residual admissible space Γ does not contain the origin, condition (14) is not fulfilled. This proved the existence of a fault.

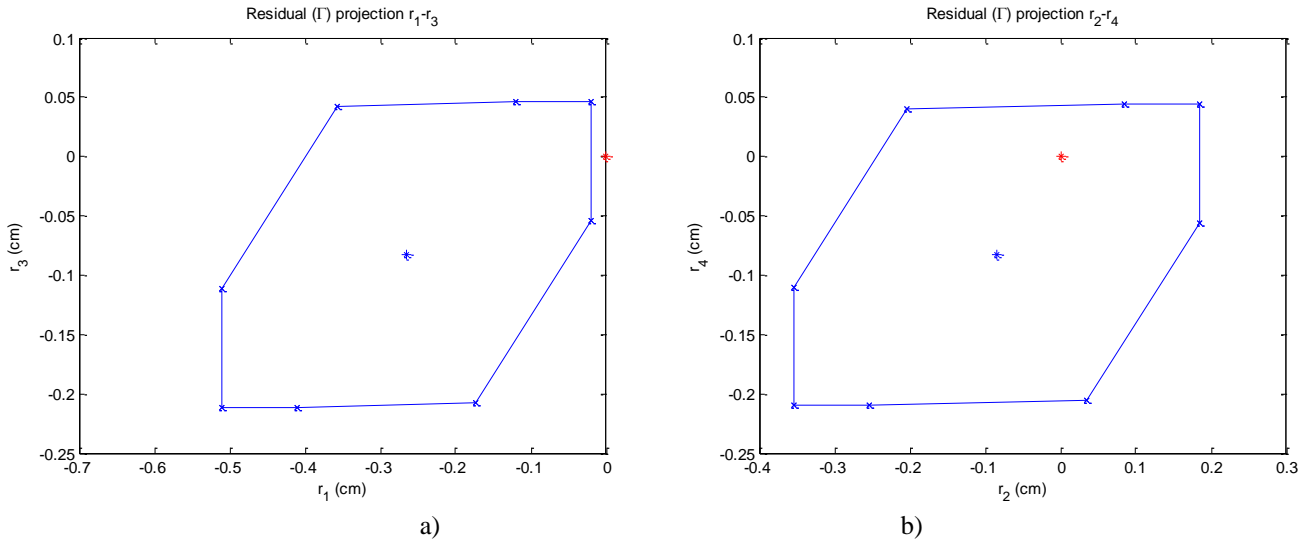


Figure 13: Residual admissible space Γ projections a) $r_1 - r_3$ and b) $r_2 - r_4$, at the fault time detection ($t=8809\text{s}$) in fault scenario 2.

Once the fault has been detected, the fault isolation and estimation procedure is activated and *Algorithm 1* is applied. Fig. 14 a) shows the evolution of the inverse of the optimisation cost function for different considered faults obtained applying *Algorithm 1* at the fault detection time ($t=8809\text{s}$) with the same window length used in the previous fault scenario.

As the objective function (J) corresponding to f_{a_1} is smaller than the objective function of the other faults considered, the fault isolation algorithm determines that the fault is a multiplicative fault affecting parameter a_1 . The fault magnitude estimation corresponding to f_{a_1} is also determined when solving *Algorithm 1* and is represented in Fig. 14 b).

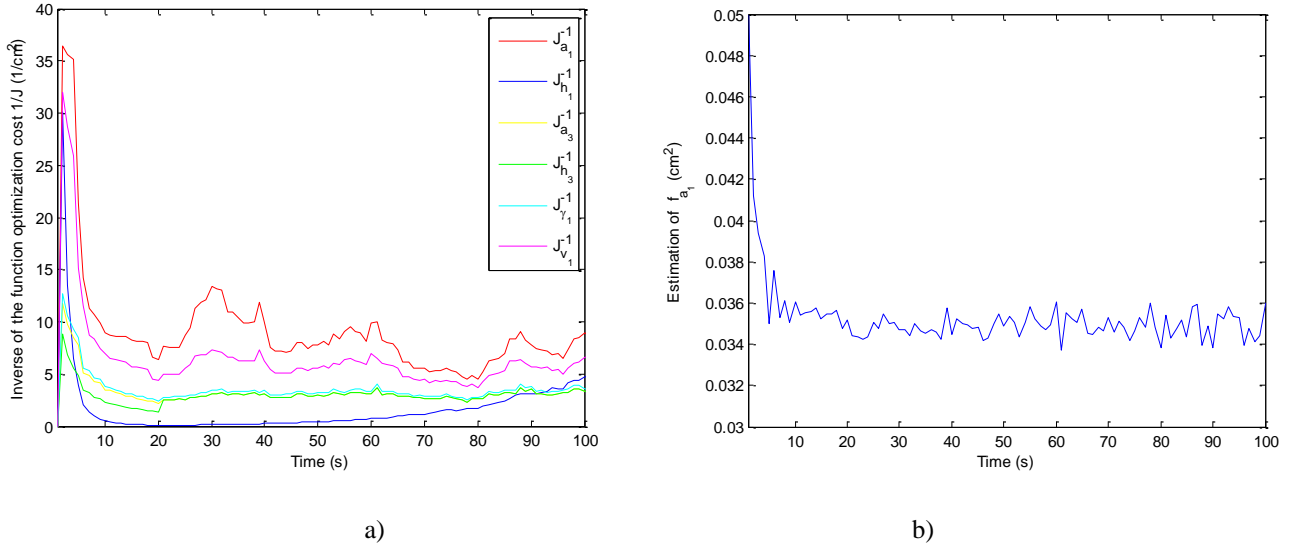


Figure 14: a) Inverse of optimisation cost function (J^{-1}) of different faults and b) fault estimation of f_{a_1} . Both figures begin in the fault time detection of fault scenario 2 ($t=8809s$).

8. CONCLUSIONS

In this paper, a robust fault detection, isolation and estimation method for systems that can be modelled by uncertain MIMO LPV models has been presented. The identification procedure is formulated as an optimisation problem that determines a zonotope that encloses the parametric uncertainty given the model structure in regressor form and additive error bounds. The fault detection methodology is based on checking if measurements are inside the prediction bounds provided by the LPV model, parametric uncertainty and additive error. It has been formulated as the feasibility problem that can be solved using linear programming algorithms. The fault isolation and estimation algorithm are based on residual fault sensitivity analysis. This methodology allows to provide additional information to the relationship between residuals and faults increasing fault isolability. Moreover, it allows obtaining a fault estimation. Finally, satisfactory results have been obtained using two case studies based on a water distribution network and a four tank system.

ACKNOWLEDGEMENTS

This work has been partially funded by the grant CICYT SHERECS DPI-2011-26243 and CICYT WATMAN DPI-2009-13744 of Spanish Ministry of Education.

REFERENCES

- Adrot, O. (2000). *Diagnostic à base de modèles incertains utilisant l'analyse par intervalles: approche bornate*. PHD thesis, Institut National Polytechnique de Lorraine, Centre de Recherche en Automatique de Nancy.
- Adrot, O. Janati-Idrissi H., Maquin D. (2002). Fault detection based on interval analysis, In *Proceedings of the 15th IFAC World Congress*. Barcelona. Spain.
- Bamieh, B., Giarré, L. (2002). Identification of linear parameter varying models. *International Journal Robust Nonlinear Control*, 2(12):841–853.
- Basseville, M., Nikiforov, I. (1993) *Detection of Abrupt Changes: Theory and Applications*, USA: Prentice Hall.
- Blanke, M., Kinnaert, M., Lunze, J., Staroswiecki, M., Schröder, J. (2006). *Diagnosis and Fault-Tolerant Control*, New York: Springer-Verlag.
- Blesa, J., Puig, V., Saludes, J. (2009). Identification for Passive Robust Fault Detection of LPV Systems using Zonotopes. In *Proceedings of 7th IFAC Symposium on Fault Detection, Supervision and Safety of Technical Processes*. Barcelona, Spain.
- Blesa, J., Puig, V., Bolea, Y. (2010). Fault detection using interval LPV models in an open-flow canal. *Control Engineering Practice*, 18 (5) 460-470.
- Blesa, J., Puig, V., Saludes J. (2011) Identification for passive robust fault detection using zonotope-based set-membership approaches. *International Journal of Adaptive Control and Signal Processing*. 25 (9) 788–812.
- Bokor, J., Szabo, Z., Stikkel, G. (2002). Failure detection for quasi LPV systems. In *Proceedings of the 41st IEEE Conference on Decision and Control*. Las Vegas, USA.
- Bokor, J. (2009). Fault Detection and Isolation in Nonlinear Systems. *IFAC Safeprocess 09. Plenary Session*. Barcelona. Spain.
- Brdys, M. A., Ulanicki, B. (1994). *Water Systems Structures, Algorithms and Applications*. Prentice Hall.
- Calafiore, G., Campi, M. C., El Ghaoui, L. (2002). Identification of reliable predictor models for unknown systems: A data-consistency approach based on learning theory. In *Proceedings of the 15th IFAC world congress*. Barcelona. Spain.
- Campi, M.C. Calafiore, G., Garatti, S. (2009). Interval predictor models: Identification and reliability. *Automatica*, Volume 45, Issue 8. pp. 382-392.
- Chen, J., Patton, R. J. (1999). *Robust model-based fault diagnosis for dynamic systems*. Kluwer Academic Publishers.
- Combastel, C. Zhang Q., Lalami A. (2008). Fault diagnosis based on the enclosure of parameters estimated with an adaptive observer. In *Proceedings of 17th IFAC World Congress*, Seoul, Korea.

- Combastel, C., Raka S.A. (2009). A Set-Membership Fault Detection Test with Guaranteed Robustness to Parametric Uncertainties in Continuous Time Linear Dynamical Systems. In *Proceedings of 7th IFAC Symposium on Fault Detection, Supervision and Safety of Technical Processes*. Barcelona, Spain.
- Ding, S. X. (2008). *Model-based Fault Diagnosis Techniques: Design Schemes, Algorithms, and Tools*. Springer.
- EPANET Programmer's Toolkit user's manual. <http://www.epa.gov>, <http://www.epanet.es/>
- Fagarasan, I., Ploix, S., Gentil, S. (2004). Causal fault detection and isolation based on a set-membership approach. *Automatica*, 40 (12). 2099-2110.
- Gertler, J. (1998) *Fault Detection and Diagnosis in Engineering Systems*. Marcel Dekker, New York.
- Henrion, D., Lasserre, J. B., Lofberg, J. (2009) GloptiPoly: Moments, Optimization and Semidefinite programming. *Optimization Methods and Software*, Vol. 24, Nos. 4-5, pp. 761-779.
- Isermann, R. (2006). *Fault-diagnosis systems: An introduction from fault detection to fault tolerance*, Berlin: Springer.
- Johansson, K.H. (2000). The quadruple-tank process: A multivariable laboratory with an adjustable zero. *IEEE Transactions on Control Systems Technology*, 8(3):456–465.
- Kwiatkowski, A., Boll, M.T., Werner, H. (2006) Automated Generation and Assessment of Affine LPV Models. In *Proceedings of the 45th IEEE Conference on Decision and Control*, San Diego, CA, USA.
- Meseguer, J., Puig, V., Escobet, T. (2010). Fault Diagnosis Using a Timed Discrete-Event Approach Based on Interval Observers: Application to Sewer Networks. *IEEE Transactions on Systems, Man and Cybernetics: Part A*, 40(5), pp. 900-916.
- Milanese, M., Norton, J., Piet Lahanier, H., Walter, E. (eds.) (1996). *Bounding approaches to system identification*. New York, USA, London, UK: Plenum Press.
- Pérez, R. Puig, V., Pascual, J., Quevedo, J., Landeros, E., Peralta, A. (2011). Methodology for Leakage Isolation using Pressure Sensitivity Analysis in Water Distribution Networks. *Control Engineering Practice*, 19(10): 1157-1167 .
- Ploix, S., Adrot, O., Ragot, J. (1999). Parameter uncertainty computation in static linear models. *Proceedings of the 38th IEEE Conference on Decision and Control*. Phoenix, Arizona.
- Ploix, S., Adrot, O. (2006). Parity relations for linear uncertain dynamic systems. *Automatica*, 42 (9), 1553-1562.
- Puig, V., Quevedo, J., Escobet, T., Nejjari, F., de las Heras, S. (2008). Passive Robust Fault Detection of Dynamic Processes Using Interval Models. *IEEE Transactions on Control Systems Technology*, 16(5), 1083 – 1089.
- Puig, V., Schmid, F., Quevedo, J. and Pulido, B. (2005). A new fault diagnosis algorithm that improves the integration of fault detection and isolation. In *Proceedings of the 44th IEEE Conference on Decision and Control, and the European Control Conference*. Seville, Spain.
- Raïssi, T. Videau G., Zolghadri A. (2010). Interval observer design for consistency checks of nonlinear continuous-time systems. *Automatica*, 46 (3), 518-527.

- Reppa V., Tzes A. (2009). Fault Detection relying on Set-Membership Techniques for an Atomic Force Microscope, In *Proceedings of the 7th IFAC Symposium on Fault Detection, Supervision and Safety of Technical Processes*. Barcelona, Spain.
- Sainz, M. Á. Armengol J., Vehí. J. (2002). Fault detection and isolation of the three-tank system using the modal interval Analysis. *Journal of Process Control*, 12 (2), 325-338.
- Shamma, J.S., Cloutier, J.R. (1993). Gain scheduled missile autopilot design using linear parameter varying transformations. *AIAA Journal of Guidance, Control, and Dynamics*, 16(2):256–263.
- Zhang, Y. M., Jiang, J. (2005). Fault diagnosis using a variable-length sliding window blockwise least-squares parameter estimation approach. In *Proc. of the 1st Workshop on Networked Control System and Fault Tolerant Control*, Ajaccio, France.

Annex 1: Uncertainty shape \mathbf{H}_0

Matrix \mathbf{H}_0 determines the weight and relations between the different parametric uncertainties. In this annex, a data-based procedure is presented to find a suitable \mathbf{H}_0 given a set of data rich enough from the identification point of view, M regressor matrix values $\Phi(k)$ and output measurements $\mathbf{y}(k)$.

Let us consider the consistency test condition (10) for all the identification data, model (1) and parameter vector $\theta(\mathbf{p}_k) \in \Theta_k$ with $\Theta_k = \theta^0(\mathbf{p}_k) + \Delta\Theta$ where $\Delta\Theta$ is a convex set. In the following, it will be described how to find the set $\Delta\Theta$ fulfilling condition (10). Notice that this parameterization of the uncertainty is more general than the parametric uncertainty given in (2) (bounded by a zonotope).

Then, the matrix \mathbf{H}_0 will be computed in such a way that the zonotope centred in the origin defined by \mathbf{H}_0 fulfils the uncertainty conditions of $\Delta\Theta$.

$$\Delta\Theta \in \mathbf{H}_0 \mathbb{B}^n \quad (61)$$

A.1 Defining convex set $\Delta\Theta$

At every instant k , the regressor matrix $\Phi(k)$ and the measured output $\mathbf{y}(k)$ define two half-spaces $\Delta\bar{\Theta}_k$ and $\Delta\underline{\Theta}_k$ in \mathbb{R}^{n_θ} that fulfil

$$\begin{aligned} \Delta\bar{\Theta}_k &= \left\{ \Delta\theta \in \mathbb{R}^{n_\theta} : \varphi_i(k)\Delta\theta \geq y_i(k) - \hat{y}_i^0(k) - \sigma_i, \forall i = 1, \dots, n_y \right\} \\ \Delta\underline{\Theta}_k &= \left\{ \Delta\theta \in \mathbb{R}^{n_\theta} : \varphi_i(k)\Delta\theta \leq y_i(k) - \hat{y}_i^0(k) + \sigma_i, \forall i = 1, \dots, n_y \right\} \end{aligned}$$

where φ_i is the i^{th} row of the regressor matrix $\Phi(k)$.

Then, the sets $\Delta\bar{\Theta}$ and $\Delta\underline{\Theta}$ that satisfy respectively $\varphi_i(k)\Delta\theta \geq y_i(k) - \hat{y}_i^0(k) - \sigma_i$ and $\varphi_i(k)\Delta\theta \leq y_i(k) - \hat{y}_i^0(k) + \sigma_i$, $\forall k = 1, \dots, M$, $\forall i = 1, \dots, n_y$ are defined by

$$\Delta\bar{\Theta} = \bigcap_{k=1}^M \Delta\bar{\Theta}_k \quad \text{and} \quad \Delta\underline{\Theta} = \bigcap_{k=1}^M \Delta\underline{\Theta}_k \quad (62)$$

Notice that: $\Delta\bar{\Theta}$ and $\Delta\underline{\Theta}$ are polytopes defined by linear inequalities.

And finally, the set $\Delta\Theta$ that fulfils condition (10) $\forall k = 1, \dots, M$ satisfies

$$\Delta\Theta \cap \Delta\bar{\Theta} \neq \emptyset \quad \text{and} \quad \Delta\Theta \cap \Delta\underline{\Theta} \neq \emptyset \quad (63)$$

Condition (63) implies that at least one point of every polytope defined in (62) belongs to the uncertainty set $\Delta\Theta$. This points will be denoted as $\Delta\bar{\theta}$ (point of $\Delta\bar{\Theta}$) and $\Delta\underline{\theta}$ (point of $\Delta\underline{\Theta}$).

In order to minimize the uncertainty of the output estimation, the parameters $\Delta\bar{\theta}$ and $\Delta\underline{\theta}$ can be chosen as follows

$$\Delta\bar{\boldsymbol{\theta}} = \arg \min_{\Delta\boldsymbol{\theta}} \sum_{k=1}^M \sum_{i=1}^{n_y} \left(\boldsymbol{\varphi}_i(k)\Delta\boldsymbol{\theta} - (y_i(k) - \hat{y}_i^0(k) - \sigma_i) \right) \quad (64)$$

subject to $\boldsymbol{\varphi}_i(k)\Delta\boldsymbol{\theta} \geq y_i(k) - \hat{y}_i^0(k) - \sigma_i \quad \forall i = 1, \dots, n_y$ and

$$\Delta\underline{\boldsymbol{\theta}} = \arg \min_{\Delta\boldsymbol{\theta}} \sum_{k=1}^M \sum_{i=1}^{n_y} \left(-\boldsymbol{\varphi}_i(k)\Delta\boldsymbol{\theta} + (y_i(k) - \hat{y}_i^0(k) + \sigma_i) \right) \quad (65)$$

subject to $\boldsymbol{\varphi}_i(k)\Delta\boldsymbol{\theta} \leq y_i(k) - \hat{y}_i^0(k) + \sigma_i \quad \forall i = 1, \dots, n_y$

A.2 Enclosing $\Delta\boldsymbol{\Theta}$ by a zonotope

Once $\Delta\bar{\boldsymbol{\theta}}$ and $\Delta\underline{\boldsymbol{\theta}}$ have been calculated, the zonotope centred in the origin that contains these two points can be determined as the box (particular case of zonotope) whose opposite vertex are $\Delta\bar{\boldsymbol{\theta}}$ and $\Delta\underline{\boldsymbol{\theta}}$ that can be defined as in (61) with \mathbf{H}_0 as

$$\mathbf{H}_0 = \text{diag} \left(H_{1;1} \quad \dots \quad H_{n_0;n_0} \right) \quad (66)$$

where $H_{i;i} = \max \left(\text{abs}(\Delta\bar{\theta}_i), \text{abs}(\Delta\underline{\theta}_i) \right) \quad i = 1, \dots, n_0$

In order to benefit of the richness of the zonotope representation of the uncertain parameter set, lets take into account possible dependencies between the different components of the parametric uncertainty, the data can be divided depending on the direction of the regressor vectors in n_D groups. Then, the parameter sets (62) can be obtained for every set of data ($\Delta\bar{\boldsymbol{\theta}}^j$ and $\Delta\underline{\boldsymbol{\theta}}^j \quad j = 1, \dots, n_D$) and, in the same way, optimal parameters ($\Delta\bar{\boldsymbol{\theta}}^j$ and $\Delta\underline{\boldsymbol{\theta}}^j \quad j = 1, \dots, n_D$) can be calculated applying (64) and (65) to every set of data.

Then, the zonotope centred in the origin that contains these $2n_D$ points can be calculated considering

$$\mathbf{H}_0 = (\kappa_1 \mathbf{v}_1, \dots, \kappa_{n_D} \mathbf{v}_{n_D}) \quad (67)$$

where $\mathbf{v}_j \quad j = 1, \dots, n_D$ are the unitary vectors (dimension $n_0 \times 1$) that define the directions of the data sets, and $\kappa_j \geq 0 \quad j = 1, \dots, n_D$ are the coefficients to be computed.

The problem of computing $\kappa_j, \quad j = 1, \dots, n_D$ can be formulated as the following linear programming optimization problem

Problem A.1: “Computation of the coefficients $\kappa_j, \quad j = 1, \dots, n_D$ ”

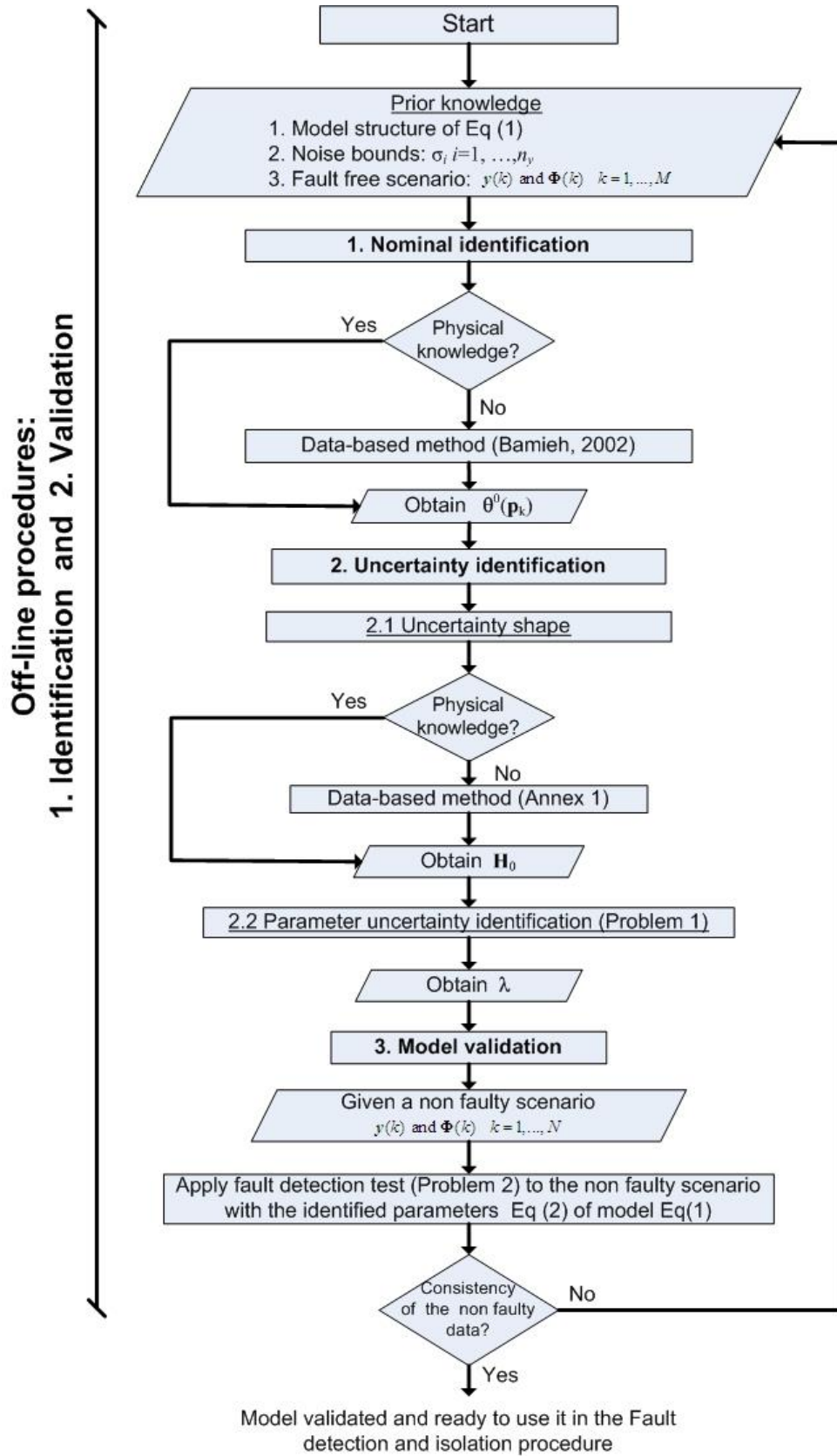
$$\min_{\kappa_i, \bar{\chi}_{i,j}, \underline{\chi}_{i,j}} \sum_{i=1}^{n_D} \kappa_i \quad \text{subject to}$$

$$\Delta \bar{\theta}^j = \sum_{i=1}^{n_D} \bar{\chi}_{i,j} \mathbf{v}_i \quad \text{and} \quad \Delta \underline{\theta}^j = \sum_{i=1}^{n_D} \underline{\chi}_{i,j} \mathbf{v}_i \quad j = 1, \dots, n_D$$

with $-\kappa_i \leq \bar{\chi}_{i,j} \leq \kappa_i$ and $-\kappa_i \leq \underline{\chi}_{i,j} \leq \kappa_i$ $i = 1, \dots, n_D, j = 1, \dots, n_D$

Notice that *Problem A.1* is a linear programming problem.

Annex 2: Off-line and on-line procedures to apply the proposed identification and fault diagnosis approach



On-line procedures:
3. Fault detection and 4. Fault Isolation and Estimation

